

Supporting Information

Tuning Emission Responses of a Triphenylamine Derivative in Host-Guest Complexes and an Unusual Dynamic Inclusion Phenomenon

*Monalisa Gangopadhyay,^a Amal K. Mandal,^c Arunava Maity,^a Sapna Ravindranathan,^b P. R. Rajamohanan,^{*b} Amitava Das^{*a}*

^a Organic Chemistry Division, ^b Central NMR Facility, CSIR-National Chemical laboratory, Pune, Maharashtra, 411008.

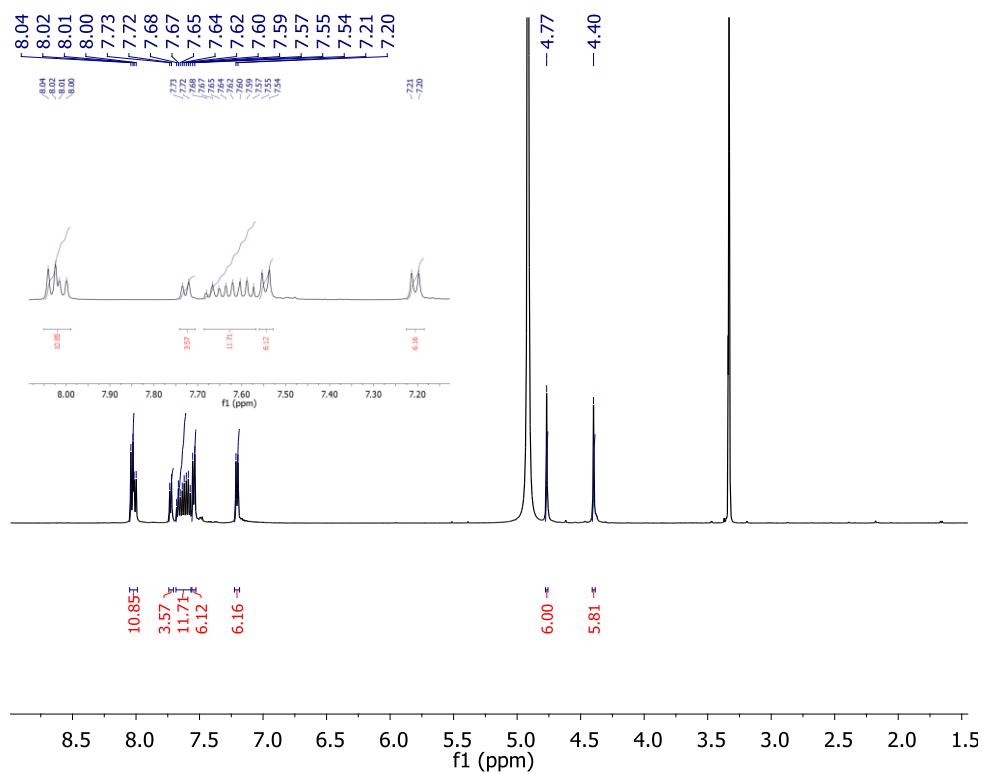
^c Molecular Nanofabrication, University of Twente Hallenweg 15, 7522 Enschede, The Netherlands.

Contents	Page no
¹ H NMR spectrum of 1 Cl ₃	2
¹³ C NMR spectrum of 1 Cl ₃	2
Mass Spectrum for 1 Cl ₃	3
IR data of 1 Cl ₃	3
Partial ¹ H NMR spectra of 1 Cl ₃ with increasing concentration of CB[7]	4
Partial ¹ H NMR spectra showing signals of neat CB[7] and [1 •3{CB[7]}]Cl ₃ complex	4
¹ H decoupled ¹³ C NMR and DEPT spectrum of [1 •3{CB[7]}]Cl ₃ complex	5
2D-COSY spectra of [1 •3{CB[7]}]Cl ₃ complex	6
2D-TCOSY spectra of [1 •3{CB[7]}]Cl ₃ complex	6
¹ H- ¹³ C HSQC spectrum of [1 •3{CB[7]}]Cl ₃ complex	7
¹ H- ¹³ C HMBC spectrum of [1 •3{CB[7]}]Cl ₃ complex	7
MALDI-TOF Mass spectrum for [1 •3{CB[7]}]Cl ₃	8
B-H plot for [1 •3{CB[7]}]Cl ₃ formation	8
2D- NOESY spectrum of [1 •3{CB[7]}]Cl ₃ complex	9
Partial ¹ H NMR spectra of 1 Cl ₃ with increasing concentration of β-CD (aromatic region)	10
¹ H decoupled ¹³ C NMR and DEPT spectrum of [1 •{β-CD}]Cl ₃ complex	10
2D-COSY spectra of [1 •{β-CD}]Cl ₃ complex	11
2D-TCOSY spectra of [1 •{β-CD}]Cl ₃ complex	11
¹ H- ¹³ C HSQC spectrum of the aliphatic region of [1 •{β-CD}]Cl ₃ complex	12
¹ H- ¹³ C HMBC spectrum of the aromatic region of [1 •{β-CD}]Cl ₃ complex	12
NOESY spectrum of [1 •{β-CD}]Cl ₃ measured at 283K	13
Expanded NOESY spectrum of [1 •{β-CD}]Cl ₃ measured at 298K	14
ROESY spectrum of [1 •{β-CD}]Cl ₃ complex at 298K	15
¹ H NMR spectra of 1 Cl ₃ , β-CD and [1 •{β-CD}]Cl ₃ complex (aliphatic region)	16
¹ H NMR spectra of [1 •{β-CD}]Cl ₃ at different temperature(aromatic region)	17
¹ H NMR spectra of [1 •{β-CD}]Cl ₃ at different temperature(aliphatic region)	18
ESI Mass spectrum of [1 •{β-CD}]Cl ₃	19
Mole ratio plot for the formation of [1 •{β-CD}]Cl ₃	19
ROESY spectra showing exchange cross peaks at 283 and 298 K	20
NOESY build up curves at different temperatures	21

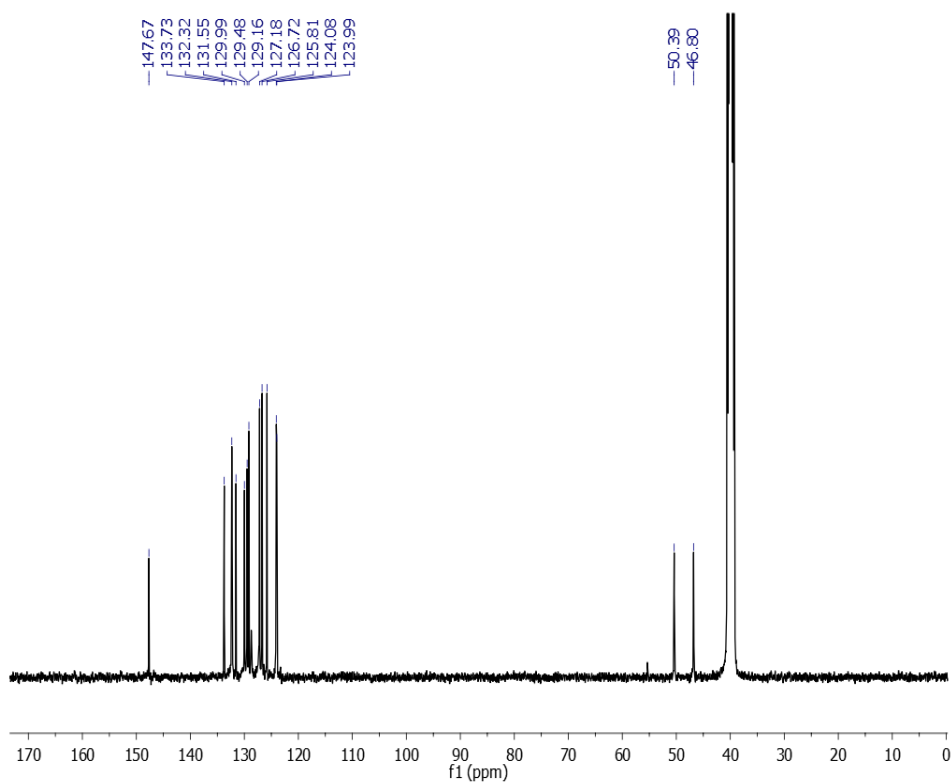
Eyring plots and calculation of thermodynamic parameters	22
Aromatic region of the ^1H NMR spectrum of $[\mathbf{1}\bullet\{\beta\text{-CD}\}]\text{Cl}_3$ complex with different $\mathbf{1Cl}_3\text{:}\beta\text{-CD}$ mole ratios	23
Comparison of the ROESY spectrum of $[\mathbf{1}\bullet\{\beta\text{-CD}\}]\text{Cl}_3$ complexes with varying $\mathbf{1Cl}_3\text{:}\beta\text{-CD}$ ratios at 298K	23
Absorbance spectra of $\mathbf{1Cl}_3$ in different solvents	24
Solvent dependent emission spectra of $\mathbf{1Cl}_3$	24
Emission spectra recorded for $\mathbf{1Cl}_3$ in water at different concentration	25
Excitation spectra of $\mathbf{1Cl}_3$ in hexane and water	25
UV-Vis Spectra of $\mathbf{1Cl}_3$ with different hosts	26
Fluorescence decay profiles	26
Details of error analyses	27
References	29

Figure S1 Spectral Characterization of **1**Cl₃ :

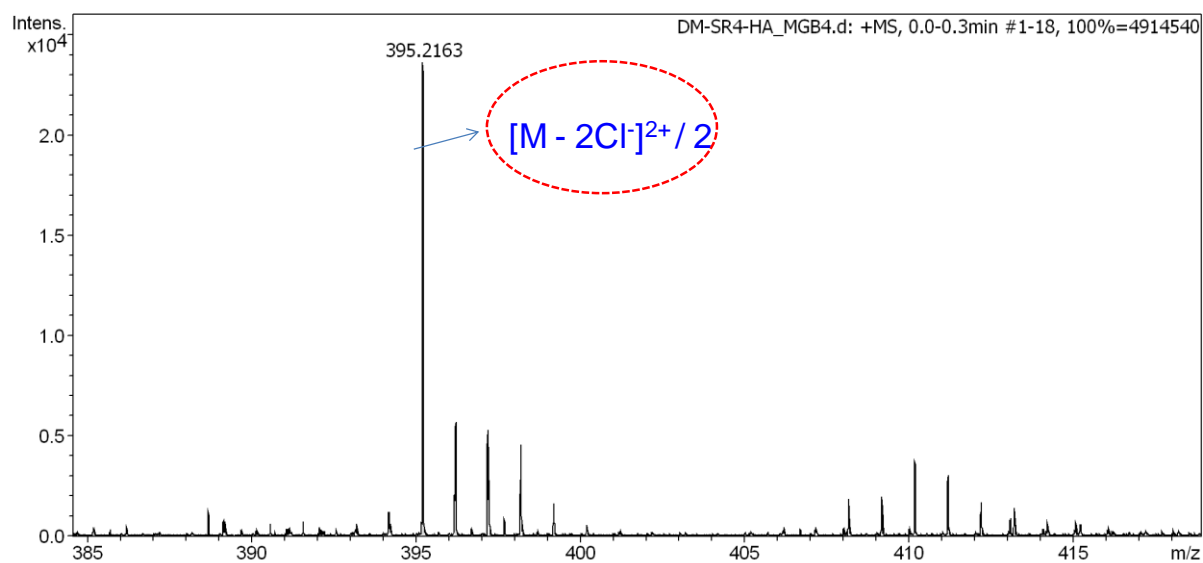
a) ¹H-NMR spectrum of **1**Cl₃ in CD₃OD at 298K



b) ¹³C-NMR spectrum of **1**Cl₃ in DMSO-d₆ at 298K



c) ESI-Mass spectrum of **1**Cl₃ in CH₃OH in positive ion mode at 298K.



d) IR spectrum of **1**Cl₃ as a KBr pellet.

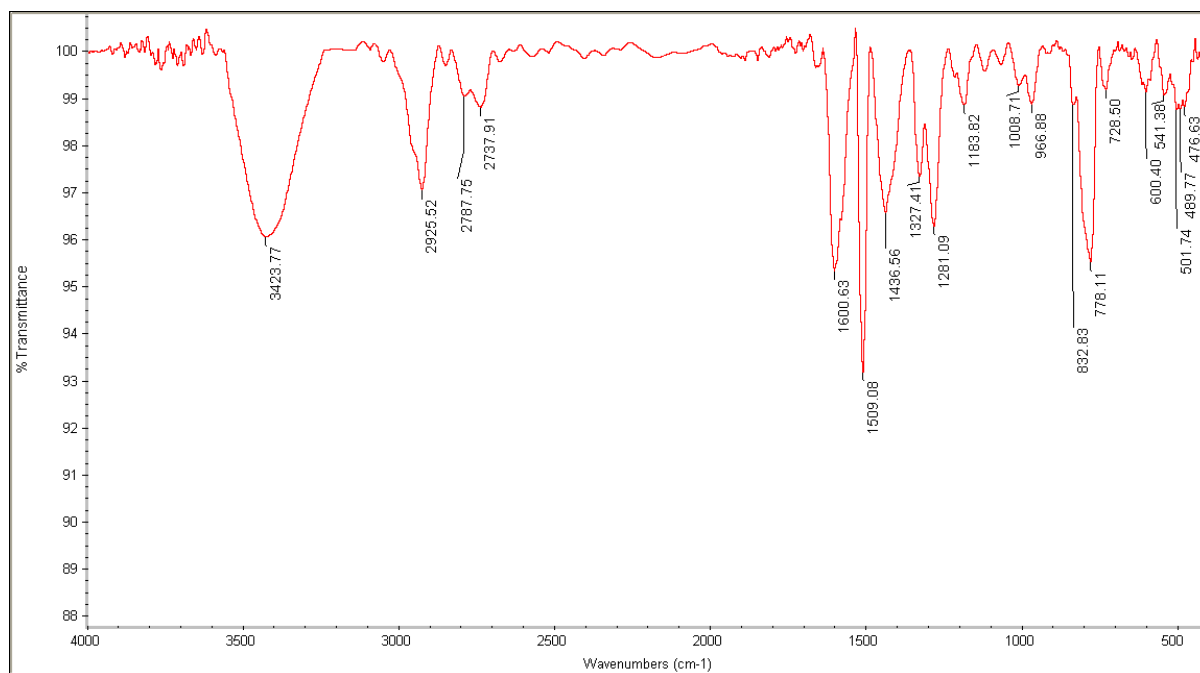


Figure S2 Partial ^1H NMR spectra (500 MHz, D_2O , 298K) of 1Cl_3 ($1.5 \times 10^{-3}\text{M}$) with varying concentrations of CB[7] (a) 0.0 mM (b) 1.5 mM (c) 3.0 mM (d) 4.5 M and (e) 9.3 mM

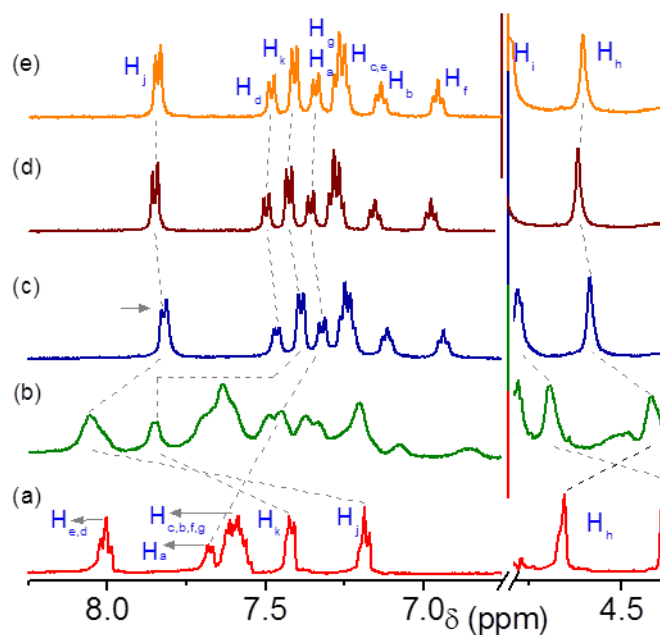


Figure S3. Splitting of signals of CB[7] in the ^1H NMR spectrum. Comparison of the aliphatic region of 700 MHz ^1H NMR spectra of CB[7] (top) and 1Cl_3 -CB[7] complex with 1.5:5 mole ratio (bottom).

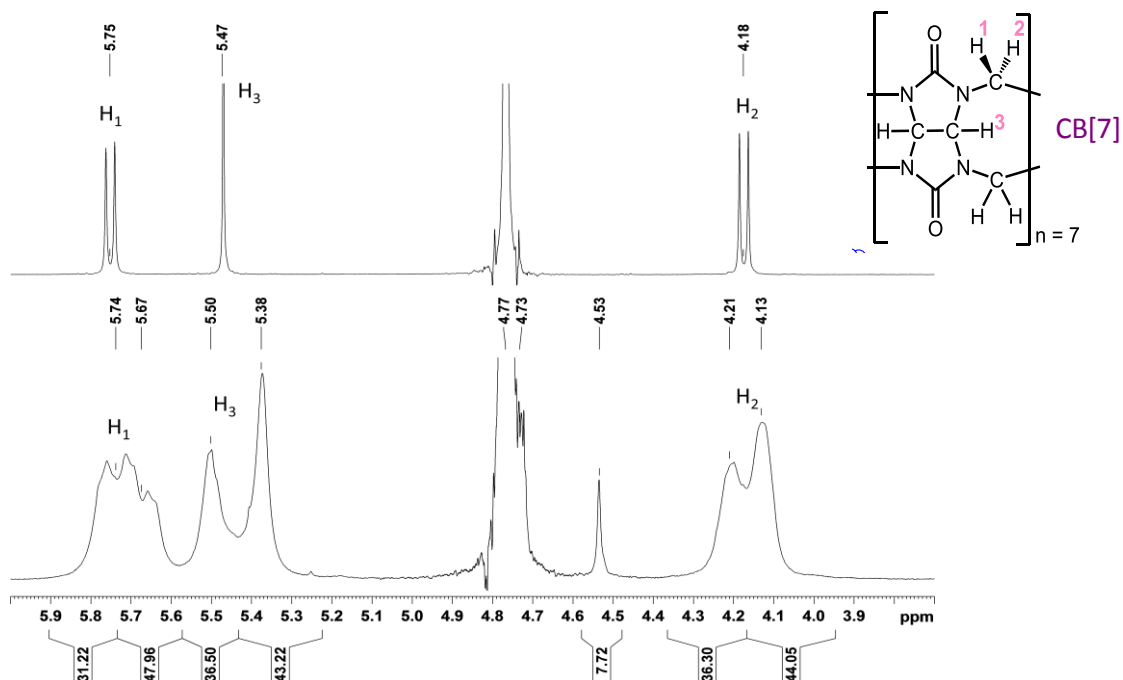


Figure S4. 175 MHz ^1H decoupled ^{13}C NMR spectrum with 23000 scans (top) and DEPT135 spectrum with 10000 scans (bottom) of $[\mathbf{1} \cdot 3\{\text{CB}[7]\}]\text{Cl}_3$ with $\mathbf{1}:\text{CB}[7]$ mole ratio 1:5.6 at 298K.

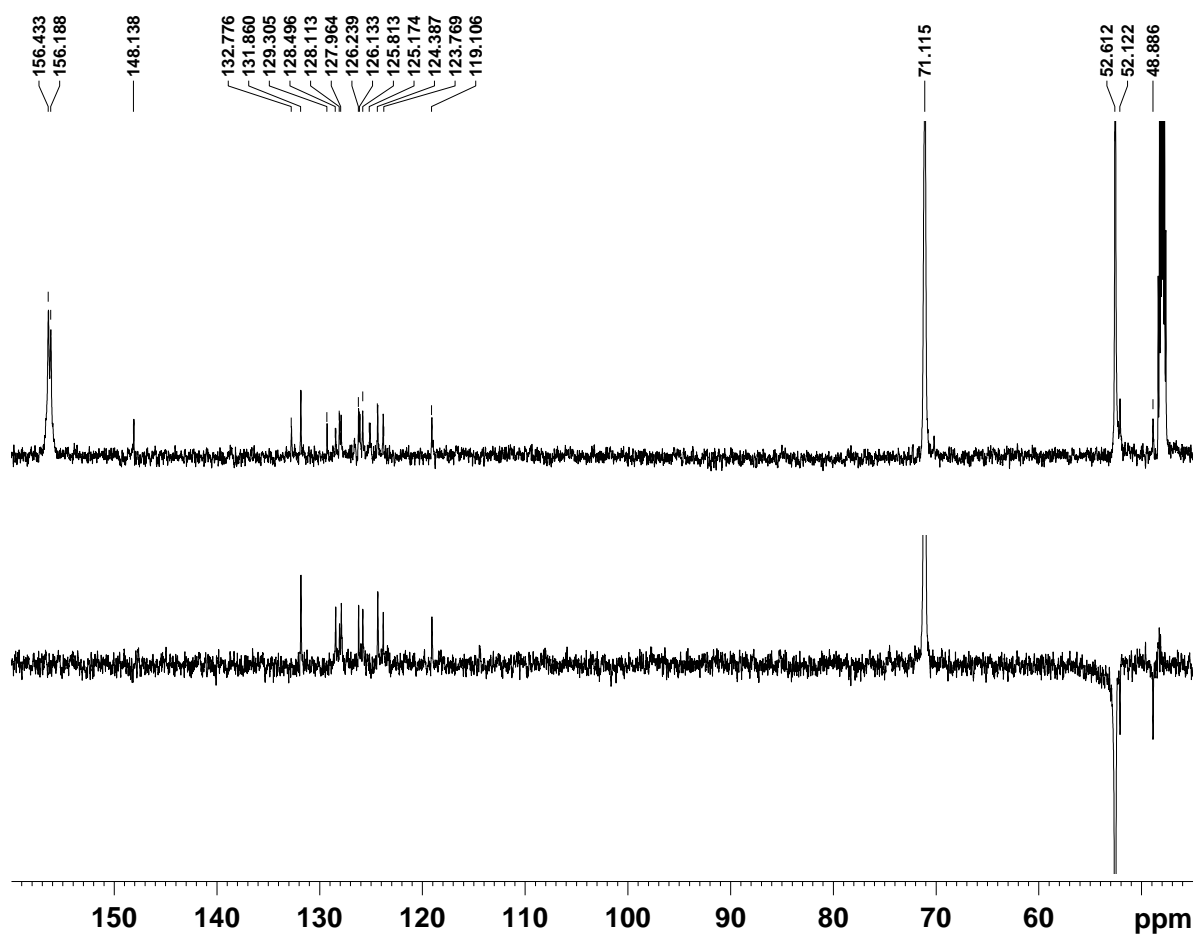


Figure S5. Aromatic region of the 700 MHz COSY (top) and TOCSY (bottom) spectra of $[\mathbf{1}\cdot\mathbf{3}\{\text{CB}[7]\}]\text{Cl}_3$. The conventional ^1H spectrum and homodecoupled pure shift ^1H spectrum are shown along F1 and F2 axis respectively. The spectra were acquired with $256 \times 2\text{K}$ data points, 16 scans and a relaxation delay of 2 s. The COSY spectrum was recorded in magnitude mode and the TOCSY spectrum was recorded in echo-antiecho mode with a mixing time of 80 ms.

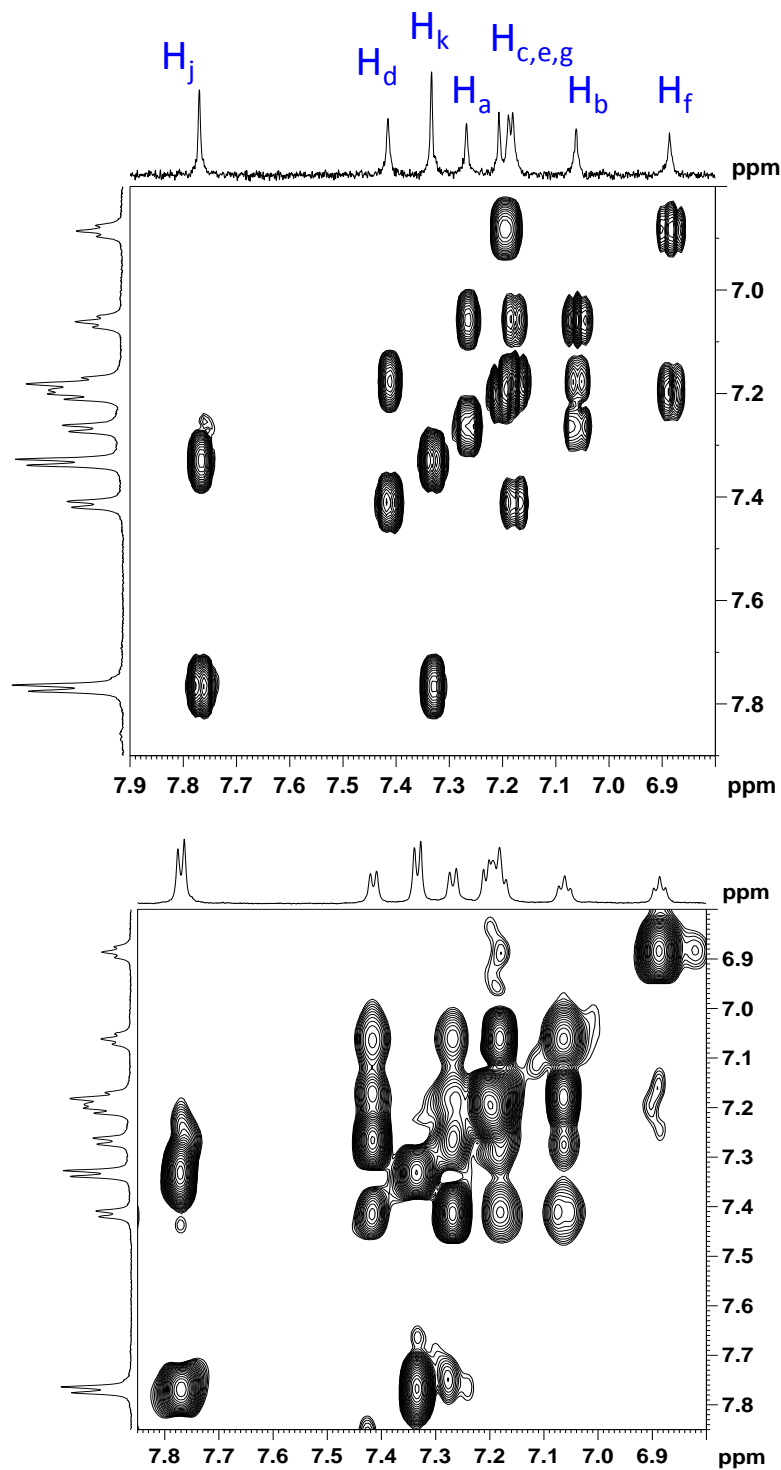


Figure S6. ^1H - ^{13}C HSQC (top) and ^1H - ^{13}C HMBC (bottom) spectra of $[\mathbf{1}\cdot\mathbf{3}\{\text{CB}[7]\}]\text{Cl}_3$. Expansion of the aromatic region of the HSQC spectrum is shown in the inset. The spectra were acquired with $140 \times 1\text{K}$ data points, relaxation delay of 2 s and number of scans 24 and 80 for HSQC and HMBC respectively.

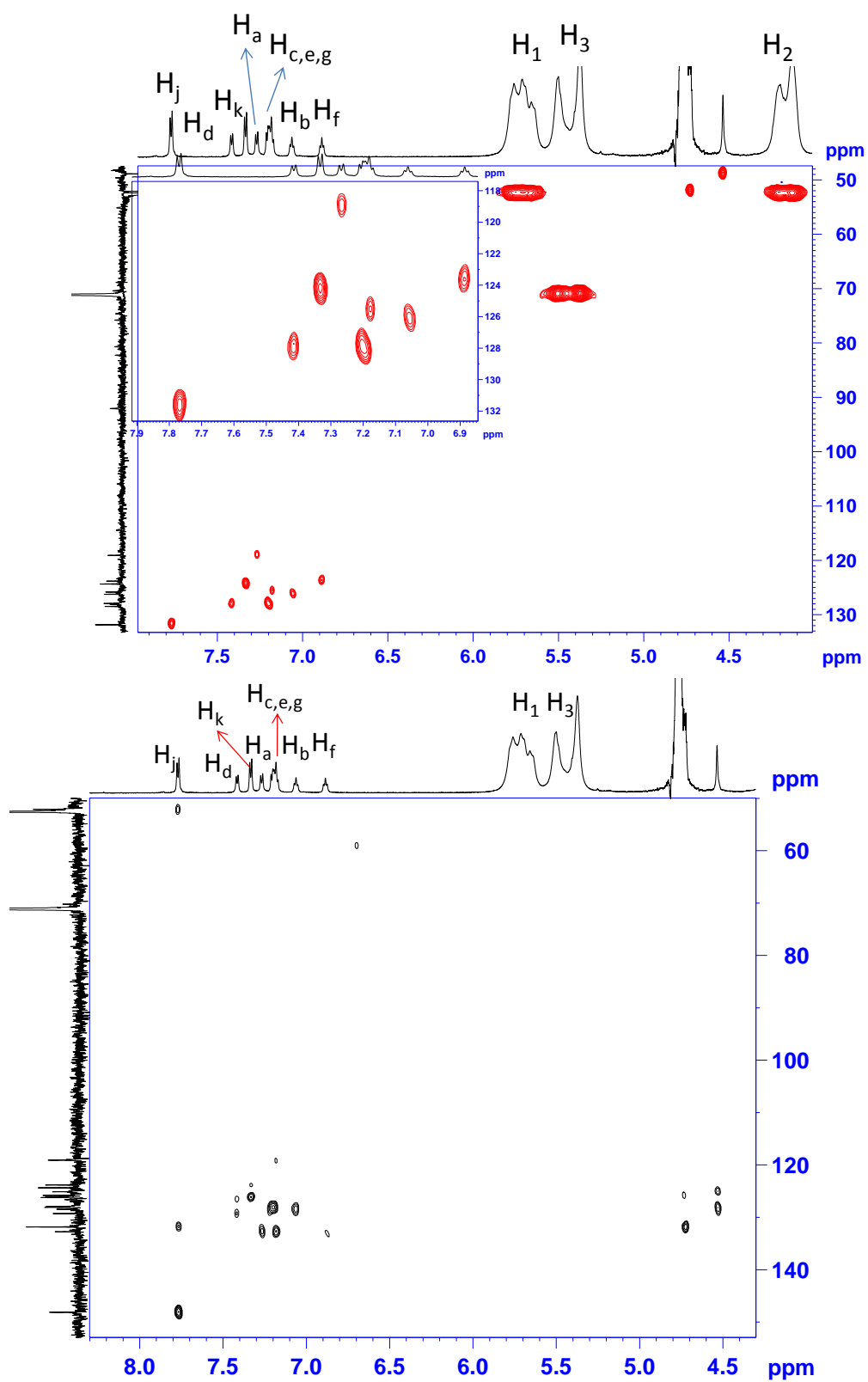


Figure S7. MALDI-TOF Mass spectrum of $[1 \bullet 3\{CB[7]\}]Cl_3$ in H_2O at 298K, with α -cyano hydroxy benzoic acid as matrix.

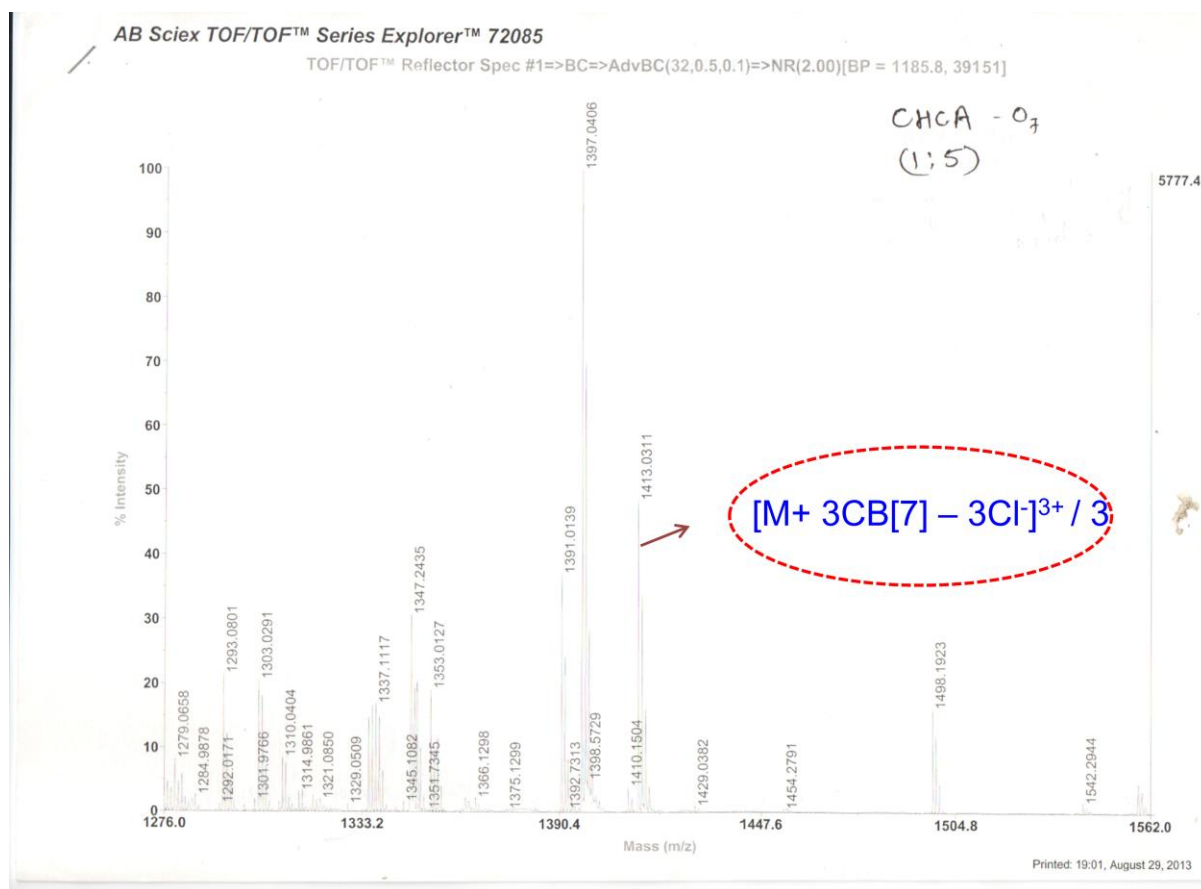


Figure S8. B-H Plot showing chemical shift changes of the H_i proton of $1Cl_3$ with $CB[7]$ concentration

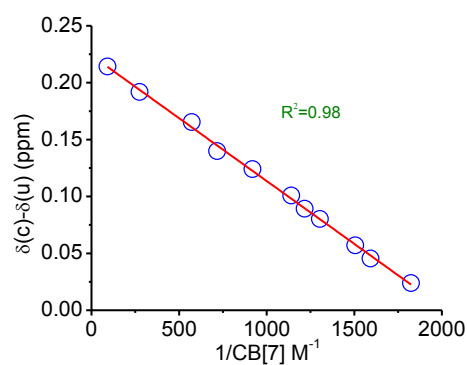


Figure S9. 700 MHz NOESY spectrum of $[\mathbf{1} \cdot 3\{\text{CB}[7]\}]\text{Cl}_3$ at 298 K. The spectrum was recorded employing a standard gradient NOESY pulse sequence in States-TPPI mode, with $256 \times 2\text{K}$ data points, 24 scans and a relaxation delay of 2s. The mixing time was set to 1 s.

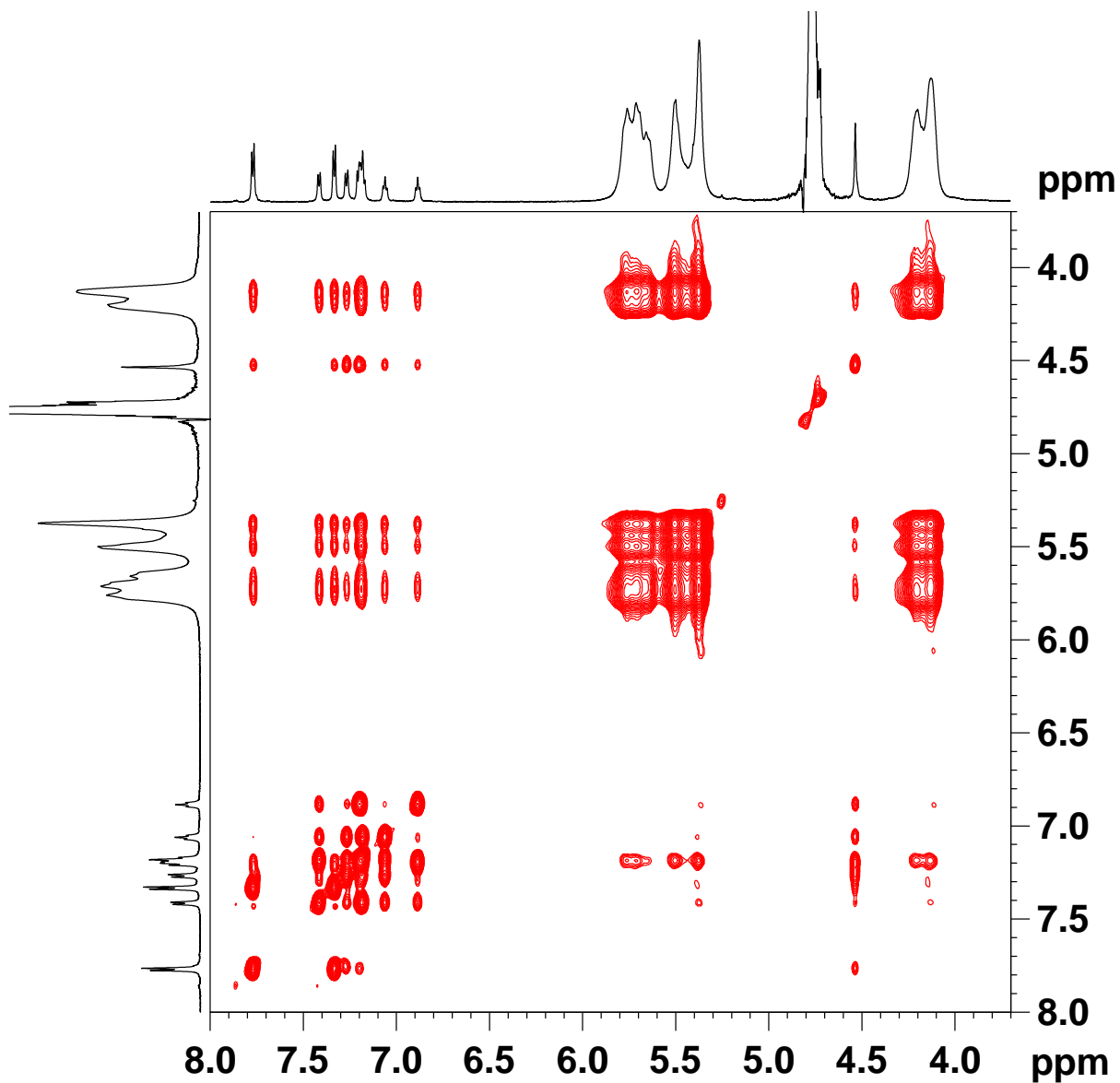


Figure S10. Partial ^1H NMR spectra (700 MHz, D_2O , 298K) of $\mathbf{1Cl}_3$ ($1.64 \times 10^{-3}\text{M}$) with varying concentrations of $\beta\text{-CD}$ (a) 0.0 mM (b) 1.0 mM (c) 3.0 mM and (d) 6.5 mM

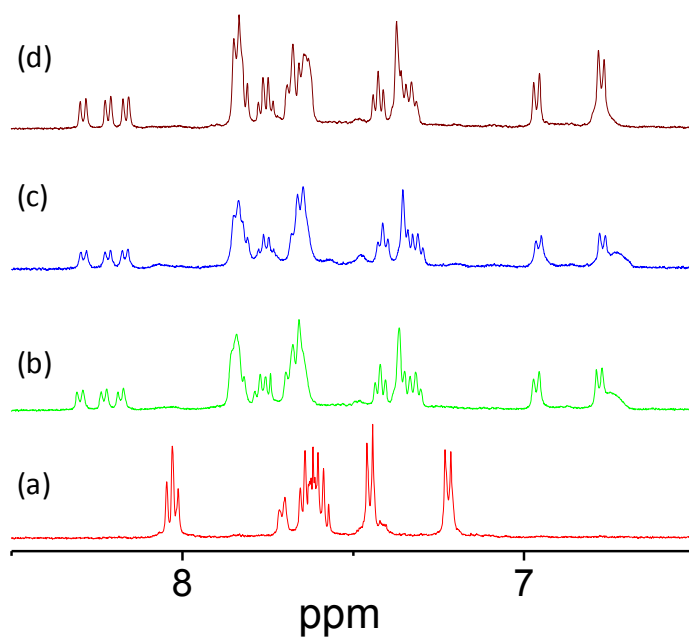


Figure S11. Aromatic region of the 175 MHz ^1H decoupled ^{13}C NMR spectrum, 30000 scans (top) and DEPT135 spectrum, 9300 scans (bottom) of $[\mathbf{1}\bullet\{\beta\text{-CD}\}]\text{Cl}_3$ with $\mathbf{1Cl}_3$: $\beta\text{-CD}$ mole ratio of 1:4 at 298K.

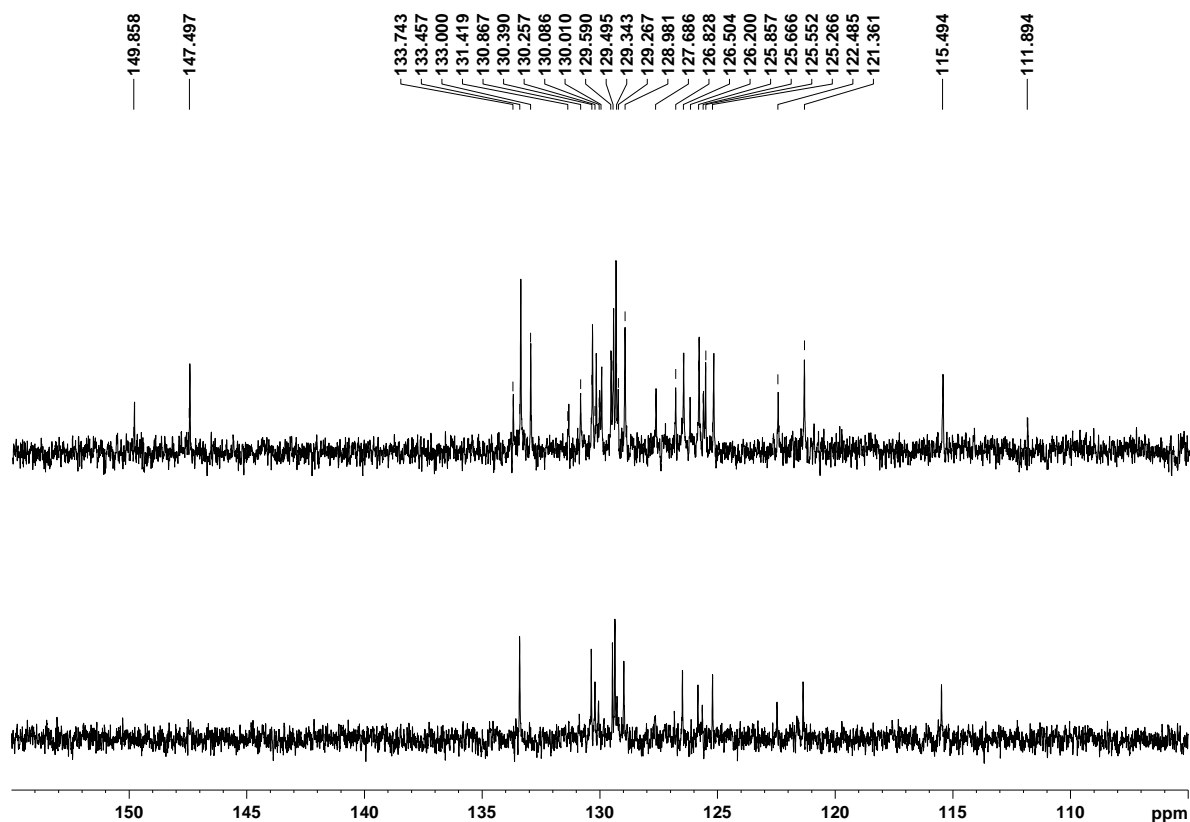


Figure S12. 700 MHz COSY spectrum of $[\mathbf{1} \cdot \{\beta\text{-CD}\}]\text{Cl}_3$ at 298K. The spectrum was recorded in magnitude mode with $256 \times 2\text{K}$ points, relaxation delay of 2 s and 16 scans.

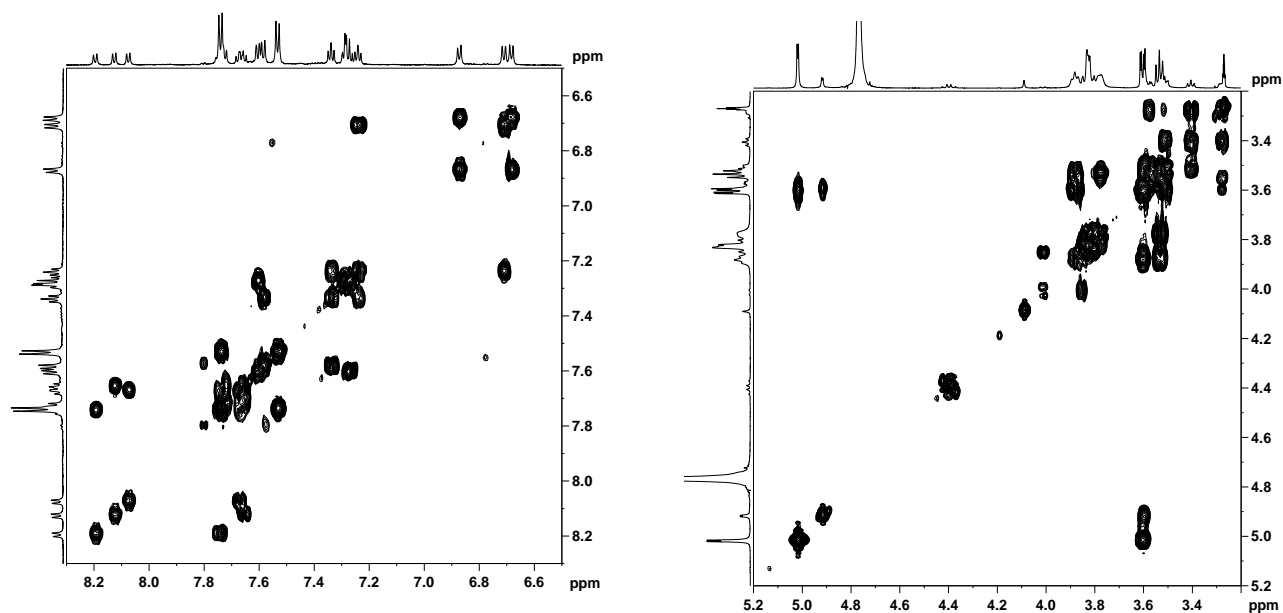


Figure S13. 700 MHz TOCSY spectrum of $[\mathbf{1} \cdot \{\beta\text{-CD}\}]\text{Cl}_3$ at 298K. The spectrum was recorded in echo-antiecho mode with $256 \times 2\text{K}$ points, relaxation delay of 2 s and 16 scans. The mixing time was set to 80ms.

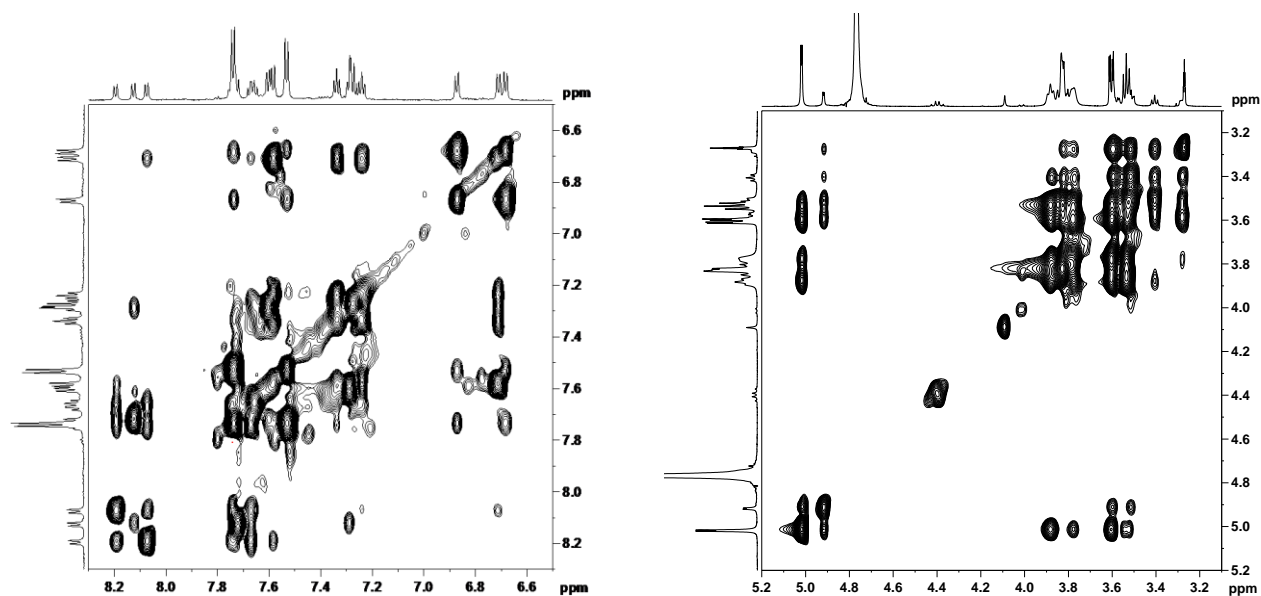


Figure S14. Multiplicity edited ^1H - ^{13}C HSQC spectrum of $[\mathbf{1}\bullet\{\beta\text{-CD}\}]\text{Cl}_3$, aliphatic region (top) and aromatic region (bottom) at 298K. The spectrum was recorded in echo-antiecho mode with $256 \times 1\text{K}$ points, relaxation delay of 2 s and 64 scans. The CH cross peaks with positive phase are shown in red while the CH_2 cross peaks with negative phase are shown in blue. The F1 and F2 projections correspond to the DEPT 135 and ^1H spectrum respectively.

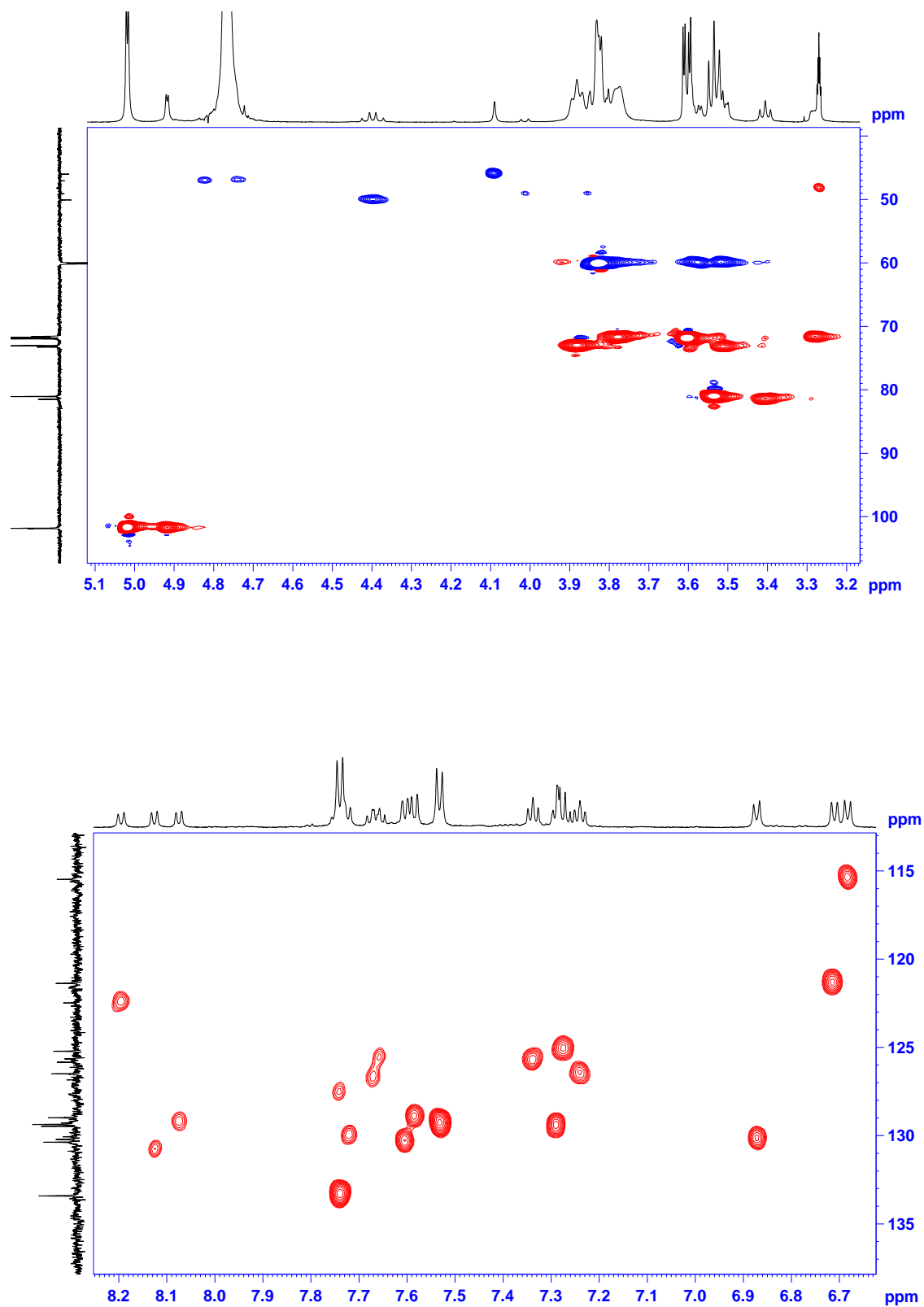
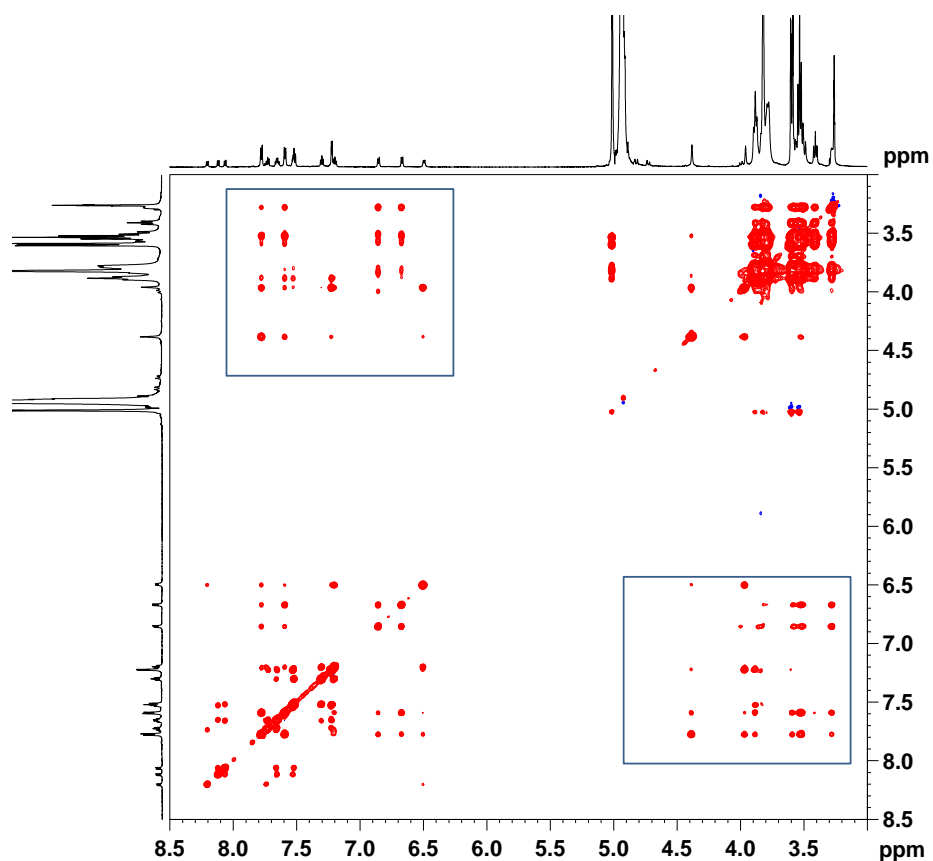


Figure S15. 700 MHz NOESY spectrum of $[1\bullet\{\beta\text{-CD}\}]\text{Cl}_3$ at 283 K. The spectrum was recorded employing a standard gradient NOESY pulse sequence in States-TPPI mode, with $256 \times 2\text{K}$ data points, 24 scans and a relaxation delay of 2s. The mixing time was set to 1 s. Crosspeaks between 1Cl3 and $\beta\text{-CD}$ arising due to complex formation are indicated in boxes.



Expansion of the aromatic (A) and aliphatic (B) regions.

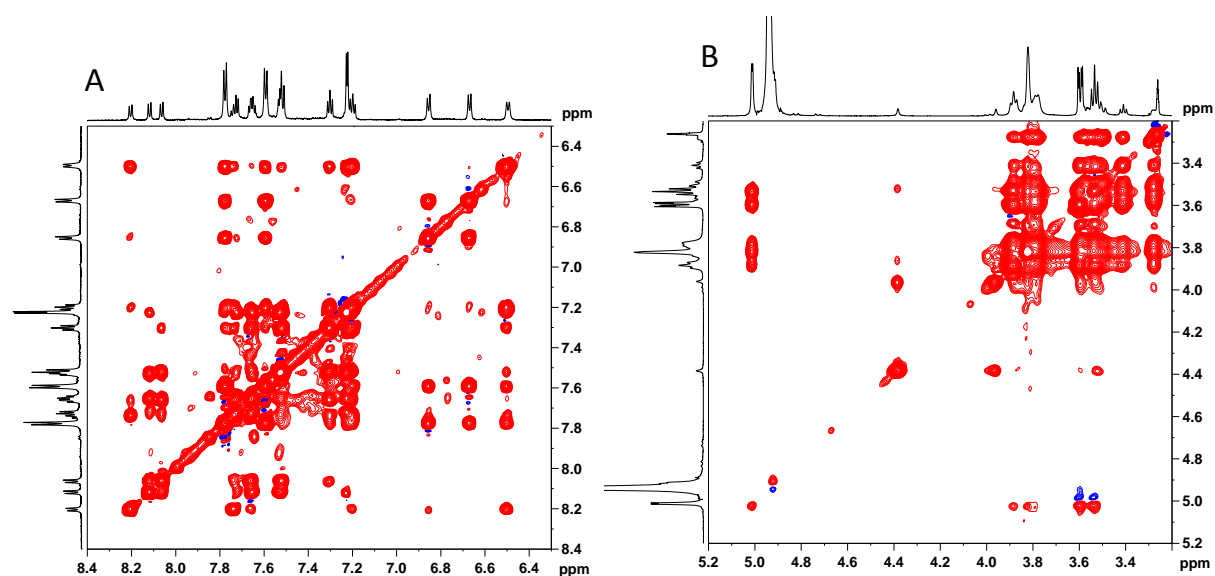


Figure S16. Part of the 700 MHz NOESY spectrum of $[\mathbf{1} \cdot \{\beta\text{-CD}\}]\text{Cl}_3$ at 298 K. Cross peaks between bound and free β -CD and aromatic protons of $\mathbf{1Cl}_3$ are indicated in boxes (top). Region showing exchange cross peaks between protons of bound and free arms of $\mathbf{1Cl}_3$ (bottom).

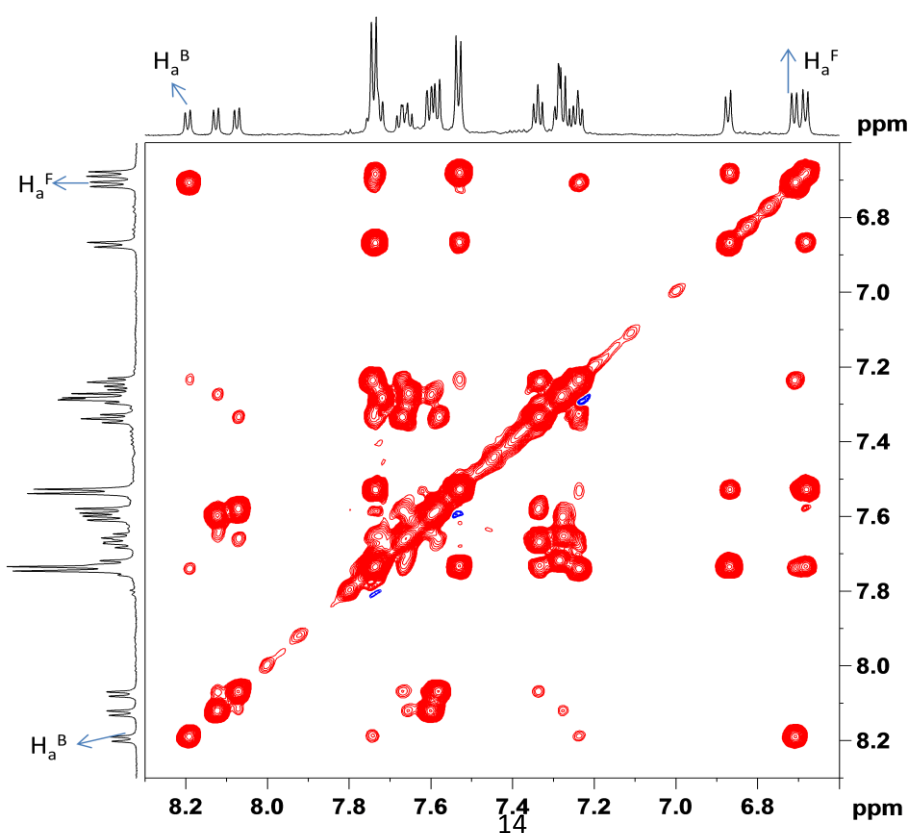
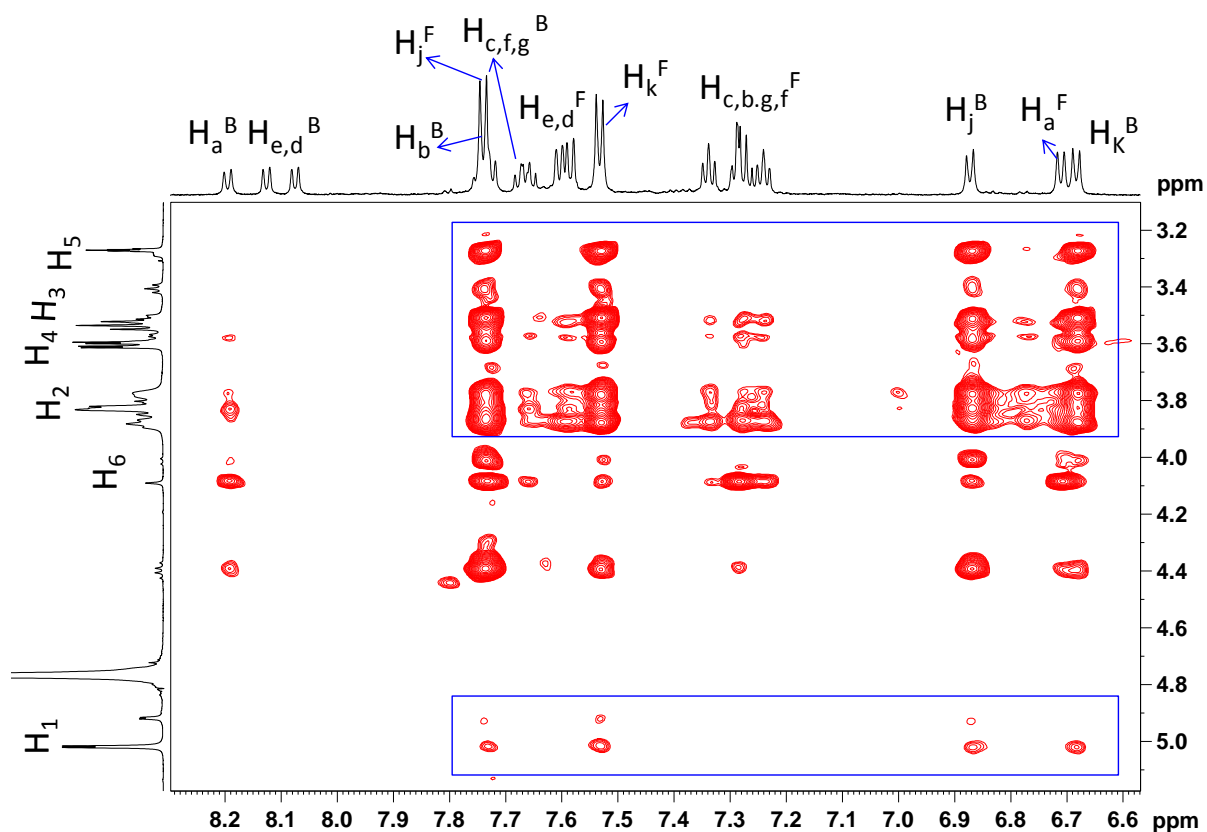
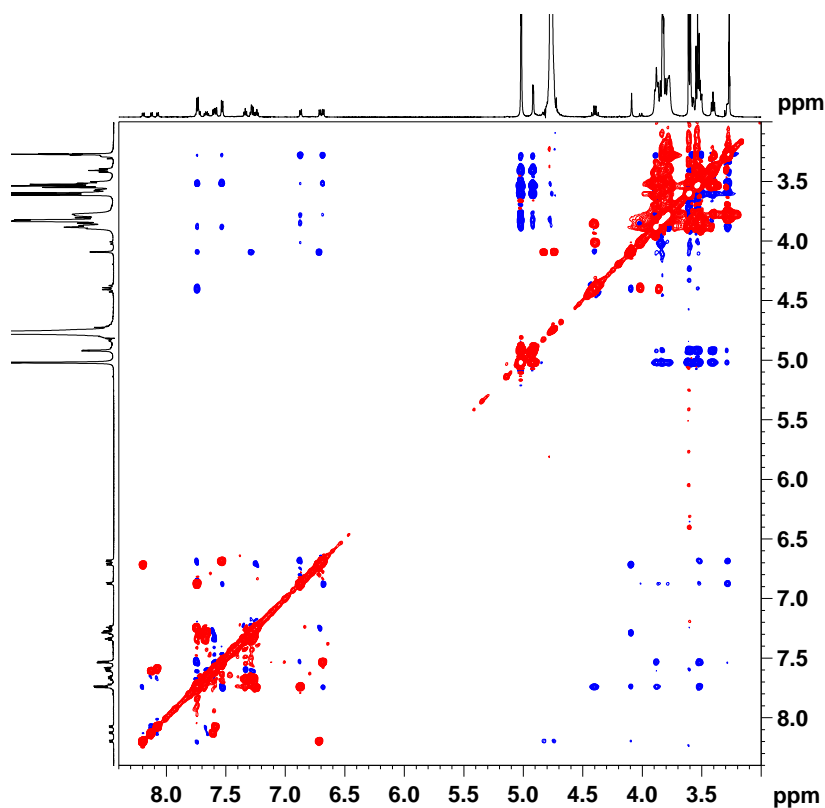


Figure S17. 700 MHz ROESY spectrum of $[\mathbf{1} \cdot \{\beta\text{-CD}\}]\text{Cl}_3$ at 298 K. The spectrum was recorded in States-TPPI mode, with $256 \times 2\text{K}$ data points, 64 scans and a relaxation delay of 3s. The mixing time was set to 250 ms. NOE and exchange cross peaks are shown in blue and red respectively.



Expansion of the aliphatic region (left). Cross peaks between the H_h and H_i (in boxes), helps to identify the signals belonging to ‘bound’ and ‘free’ arms of $\mathbf{1Cl}_3$. Expansion of the region showing intermolecular NOE contact (right). NOE crosspeaks of H_j and H_k protons of ‘free’ and ‘bound’ arms of $\mathbf{1Cl}_3$ to H_5 proton of $\beta\text{-CD}$ in the complex are highlighted by red and black boxes respectively. The intra-arm NOE cross peaks are shown in circles.

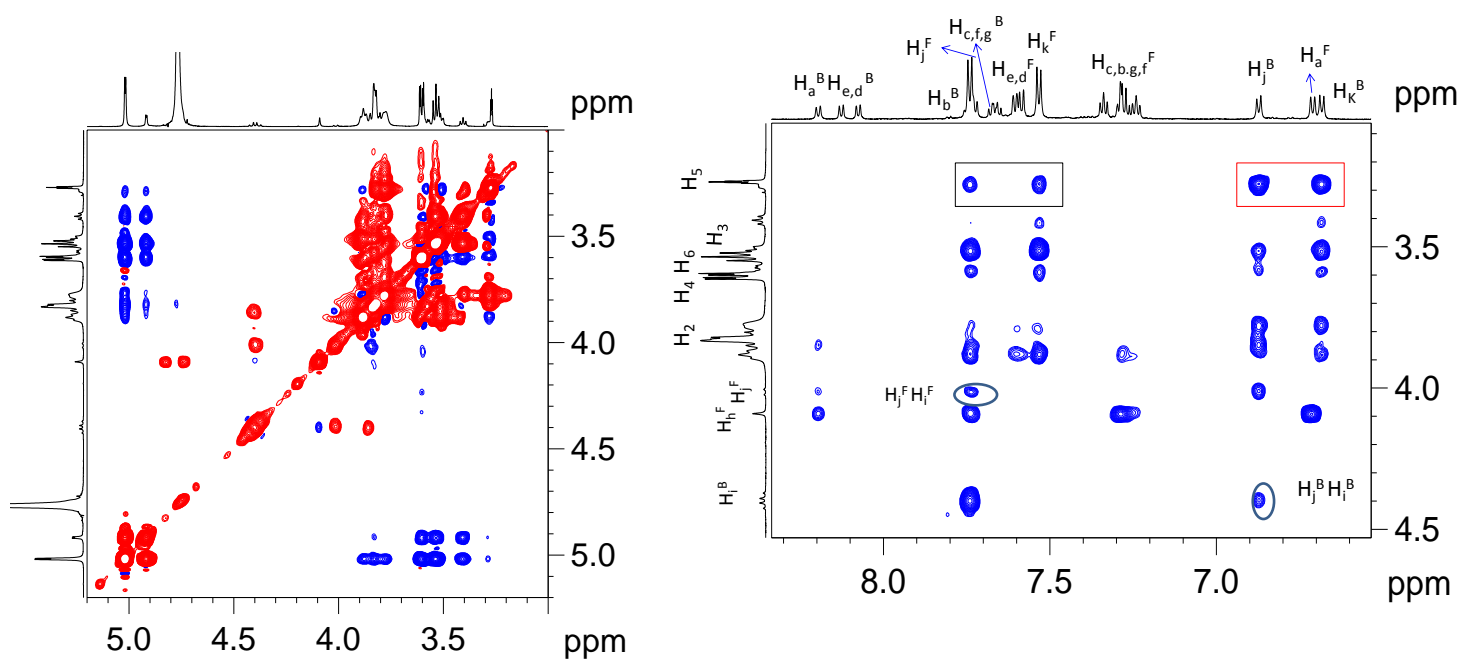


Figure S18. 700 MHz ^1H NMR spectra of $\mathbf{1Cl}_3$ (bottom), $\beta\text{-CD}$ (center) and $[\mathbf{1}\cdot\{\beta\text{-CD}\}]\text{Cl}_3$ complex at 1:4 mole ratio (top). Signals of bound $\beta\text{-CD}$ are marked with an asterisk. Signals from the ‘bound’ and ‘free’ arms of $\mathbf{1Cl}_3$ in the complex are indicated by ‘B’ and ‘F’ respectively.

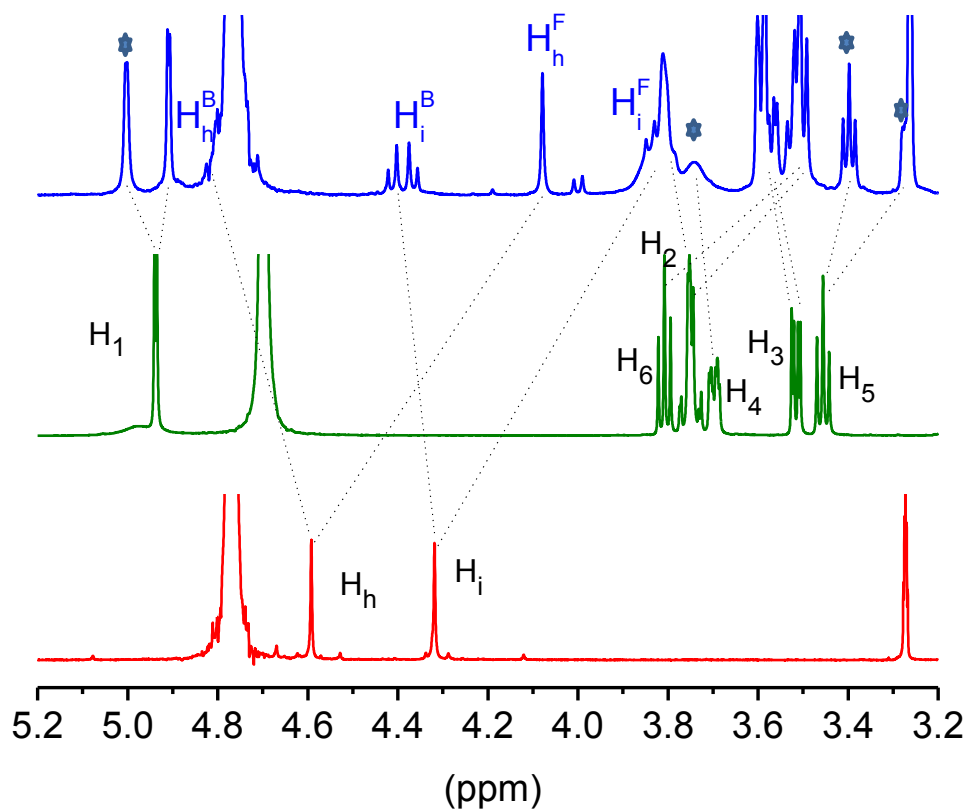


Figure S19. Aromatic region of the variable temperature ^1H NMR spectra (700 MHz) of the $[\mathbf{1}\bullet\{\beta\text{-CD}\}]\text{Cl}_3$ complex with $\mathbf{1}\text{Cl}_3\text{:}\beta\text{-CD}$ mole ratio of 1:4.

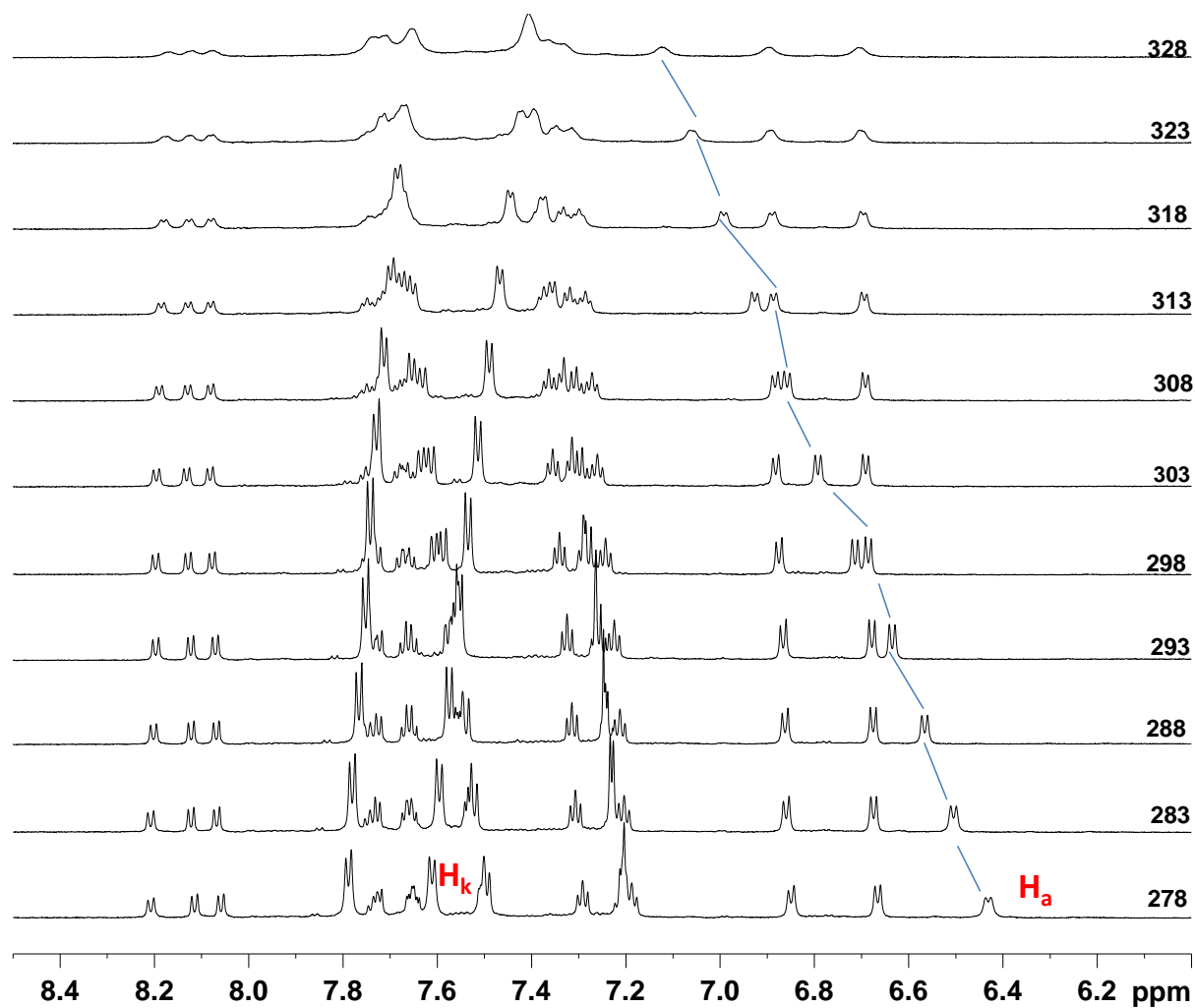


Figure S20. Aliphatic region of the variable temperature ^1H NMR spectra (700 MHz) of the $[\mathbf{1} \cdot \{\beta\text{-CD}\}]\text{Cl}_3$ complex with $\mathbf{1}:\text{Cl}_3:\beta\text{-CD}$ mole ratio of 1:4.

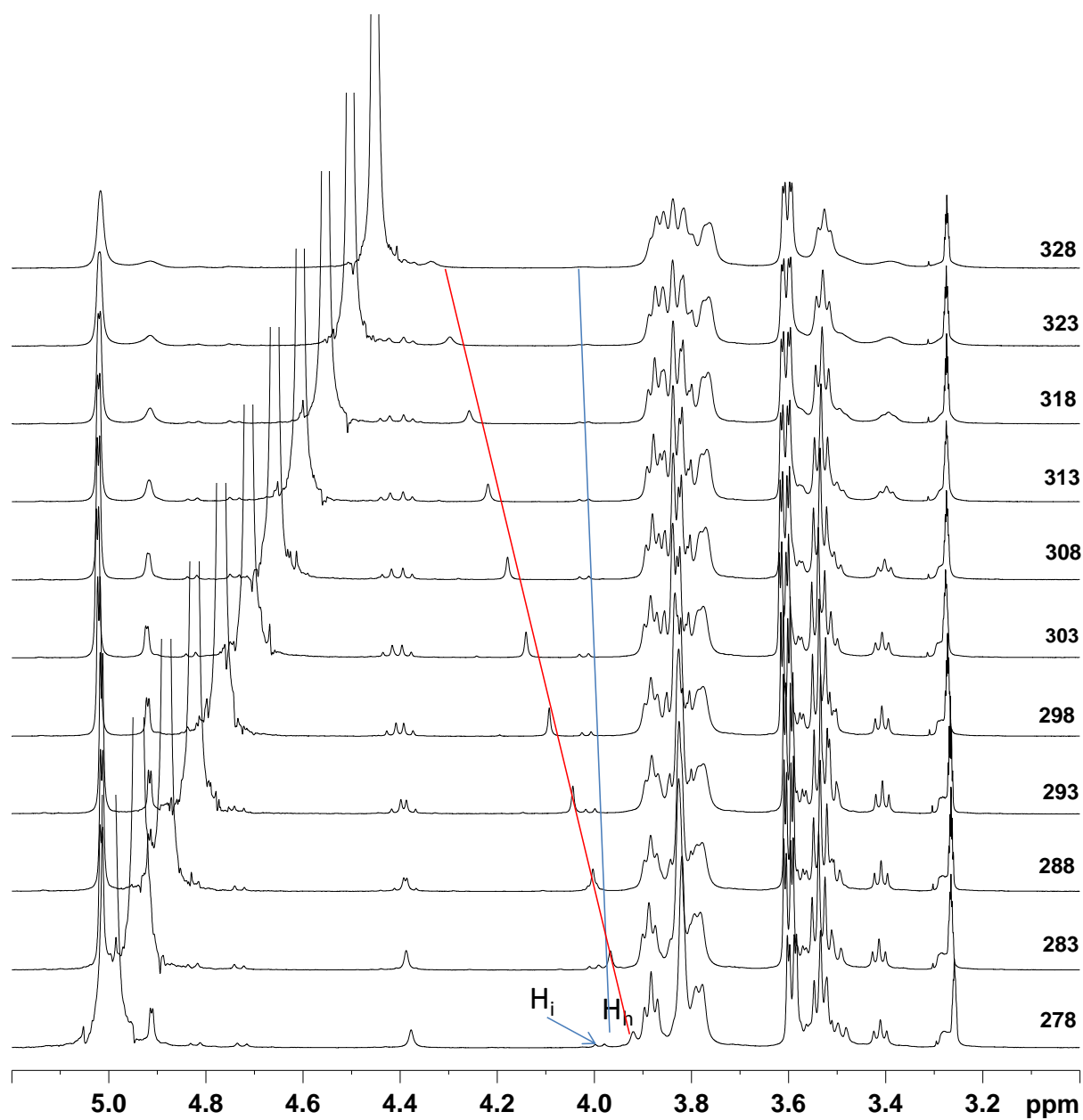


Figure S21. ESI Mass spectrum of $[1 \bullet \{\beta\text{-CD}\}]\text{Cl}_3$.

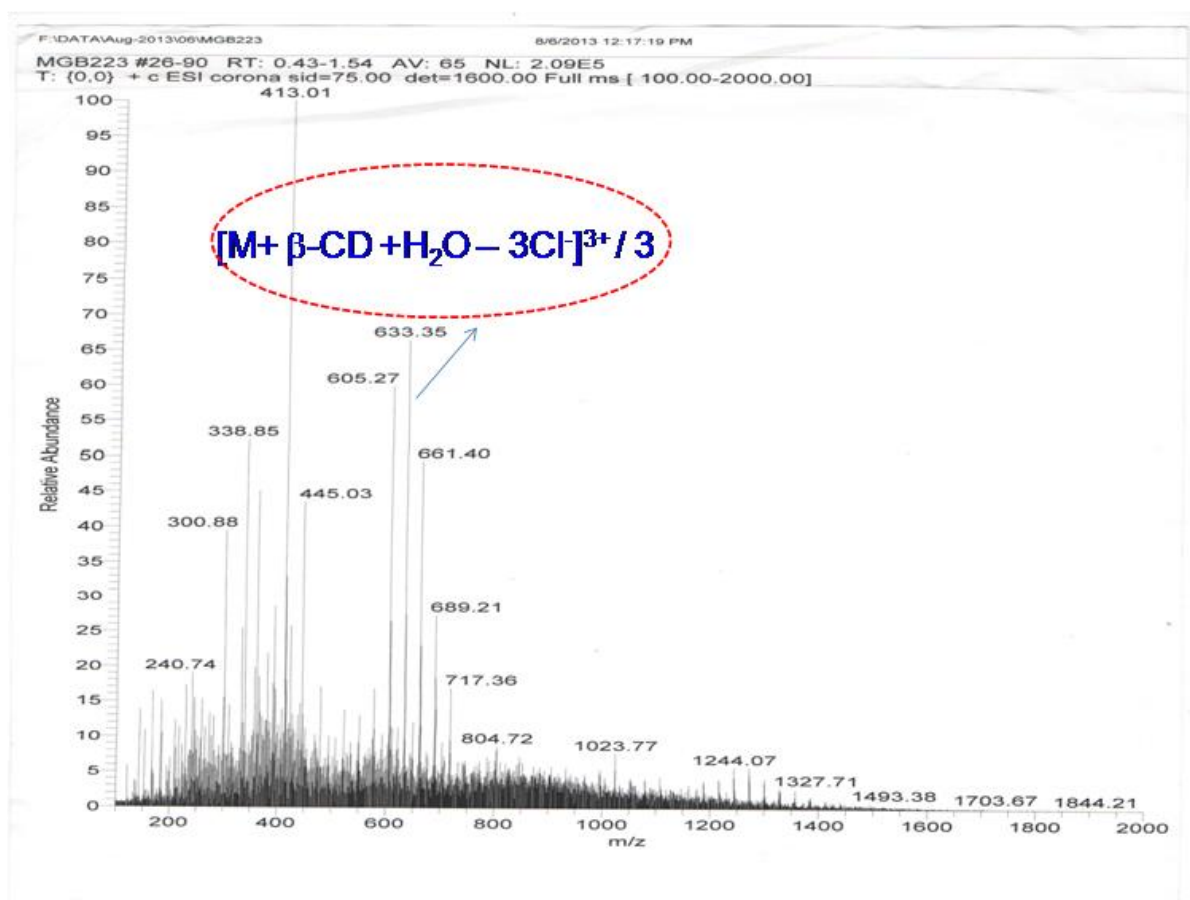


Figure S22. Mole ratio plot analysis of the formation of $[1 \bullet \{\beta\text{-CD}\}]\text{Cl}_3$ complex.

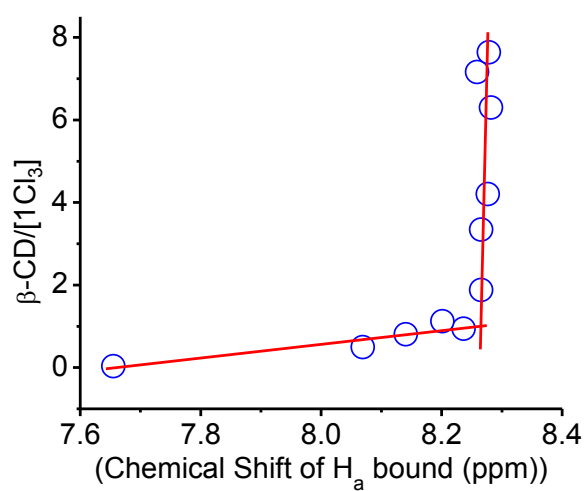


Figure S23. 700 MHz ROESY spectra of $[1 \cdot \{\beta\text{-CD}\}] \text{Cl}_3$ at 298 K (left) and 283 K (right). Exchange cross peaks between the H_a protons of the ‘bound’ and ‘free’ arms of 1Cl_3 in the complex are indicated by circles and the corresponding pairs for the H_j and H_k protons are indicated by squares.

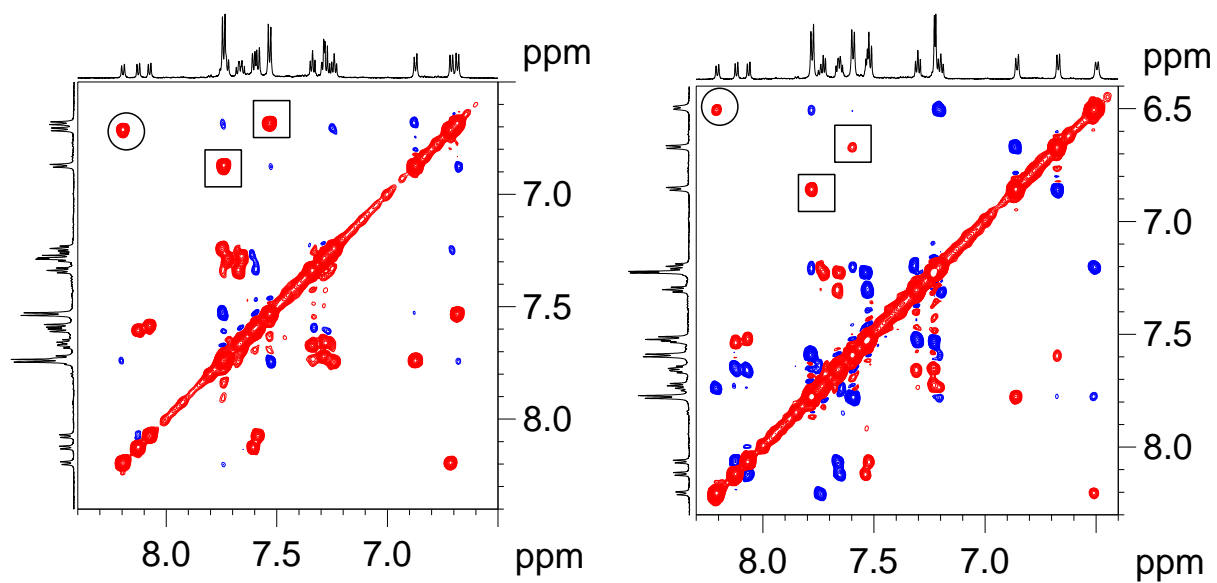
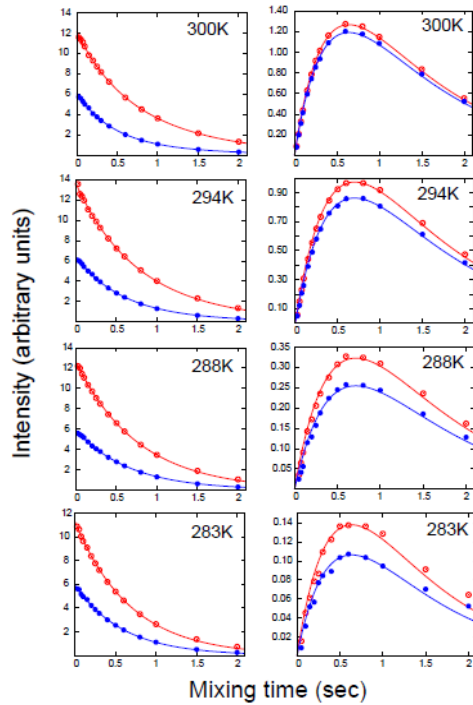


Figure S24. NOE decay and build-up curves measured at different temperatures for the H_a proton of **1**Cl₃ in the [**1**•{β-CD}]Cl₃ complex on a 700 MHz spectrometer. The symbols are experimental data (red: H_a from the ‘free’ arm, blue: H_a from the ‘bound’ arm) and solid lines represent fits based on equation 2.



Analysis of two site exchange by 2D exchange spectroscopy

The observed two site exchange may be represented as $A \rightleftharpoons B$, where A and B corresponds to a proton in the ‘free’ and ‘bound’ arm of **1**Cl₃ in the ([**1**•{β-CD}]Cl₃) complex.

The evolution of longitudinal magnetization in 2D exchange spectroscopy is described by^[1,2],

$$\frac{d}{dt} \begin{bmatrix} m_a(t) \\ m_b(t) \end{bmatrix} = \begin{bmatrix} -R_{1a}^0 - k_f & k_r \\ k_f & -R_{1b}^0 - k_r \end{bmatrix} \begin{bmatrix} m_a(t) \\ m_b(t) \end{bmatrix} \quad (1)$$

where $m_a(t) = M_{zA}(t) - M_A^0$ and $m_b(t) = M_{zB}(t) - M_B^0$ represent deviations of the magnetization from equilibrium, k_f and k_r are the forward and backward rate constants respectively and R_{1a}^0 and R_{1b}^0 are the longitudinal relaxation rates in the two states. The solution to the matrix equation is given by,

$$\mathbf{m}(\tau_m) = \mathbf{X} \exp(-\mathbf{D}\tau_m) \mathbf{X}^{-1} \mathbf{m}(0) \quad (2)$$

where \mathbf{D} is the diagonal matrix of the eigenvalues of the rate matrix in equation 1 and \mathbf{X} is the matrix of the corresponding eigenvectors. The intensities of the diagonal (decay curves) and cross peaks (build-up curves) as a function of mixing time τ_m , measured in the 2D exchange experiment are fit simultaneously to equation 2 to extract the parameters k_f , k_r , R_{1a}^0 , R_{1b}^0 , m_a^0

and m_b^0 where the latter (m_a^0, m_b^0) correspond to the intensities of the diagonal peaks at zero mixing time.

Table S1. Parameters determined from the fits of decay and build-up curves obtained from the NOE exchange experiment to equation 2.

T, K	k_f, s^{-1}	k_r, s^{-1}	R_{1a}^0, s^{-1}	R_{1b}^0, s^{-1}	m_a^0	m_b^0
283	0.0524±0.007	0.0767±0.014	1.4149±0.011	1.6026±0.024	1126930±2730	593168±2856
288	0.0975±0.005	0.1645±0.010	1.2077±0.007	1.3438±0.017	1261660±2087	590031±2183
294	0.2824±0.008	0.5313±0.017	1.0088±0.011	1.1224±0.027	1360930±3658	641326±3918
300	0.4573±0.007	0.8596±0.014	0.9103±0.009	1.0972±0.022	1212580±2466	606549±2734

Table S2. Equilibrium constants calculated from exchange parameters determined from 2D exchange experiments

T, K	K_0
283	0.6832±0.16
288	0.5927±0.05
294	0.5315±0.02
300	0.5319±0.01

The thermodynamic parameters associated with the exchange process were determined based on the Eyring equation,

$$\ln\left(\frac{K_0}{T}\right) - \ln\left(\frac{k_B}{h}\right) = \frac{\Delta S}{R} - \frac{\Delta H}{RT} \quad (3)$$

where K_0 is the equilibrium constant. k_b is the Boltzmann constant, h is the Planck's constant and R is the gas constant. From a plot of the LHS of equation 3 vs $1/T$, ΔH and ΔS were estimated from the slope and intercept respectively.

Figure S25. Eyring plot for estimation of ΔH and ΔS .

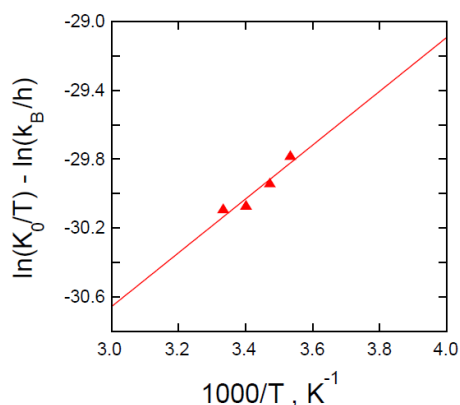


Figure S26. Aromatic region of the 700 MHz ^1H NMR spectrum of 1Cl_3 and the complex with $\beta\text{-CD}$ for $1\text{Cl}_3:\beta\text{-CD}$ mole ratios of 1:0, 1:0.3, 1:0.65, 1:2 and 1:4 at 298K. Signals belonging to unbound 1Cl_3 (ex: ~ 7.9 ppm) decreases as $\beta\text{-CD}$ concentration increases and is almost absent at a mole ratio of 1:4.

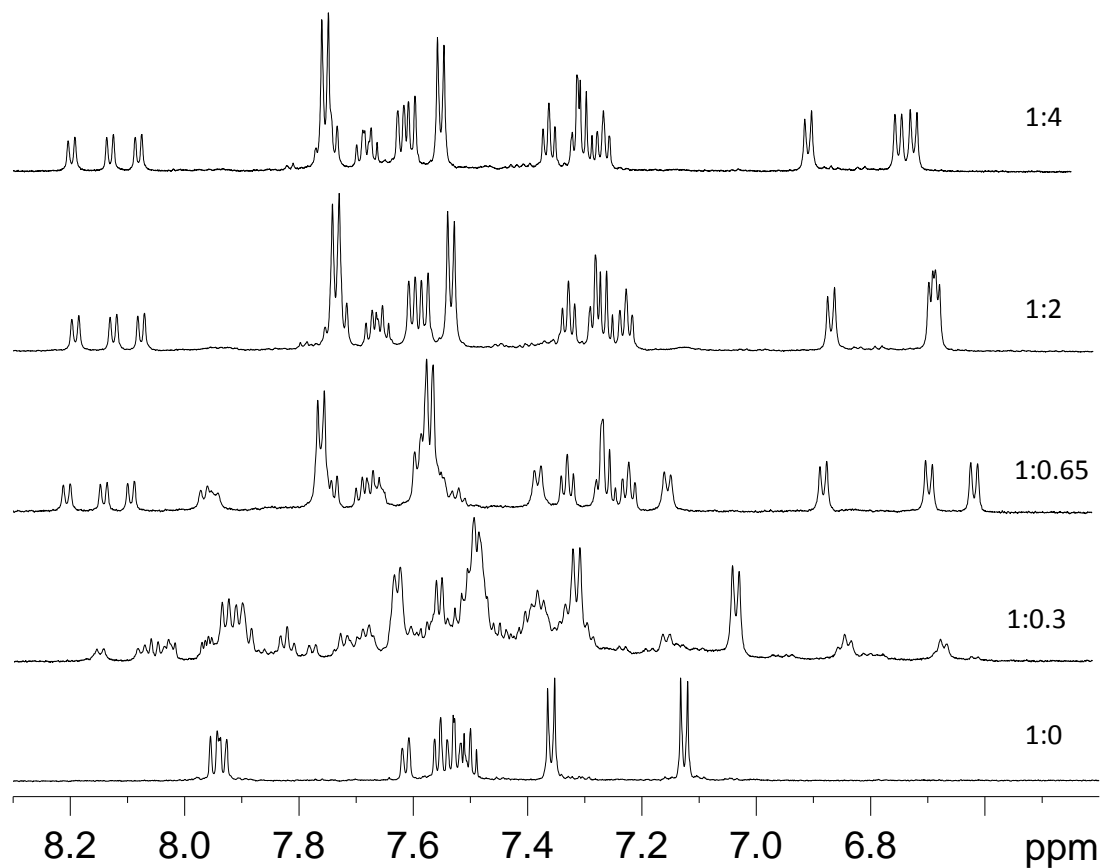


Figure S27. 700 MHz ROESY spectra of $[1\bullet\{\beta\text{-CD}\}]\text{Cl}_3$ at 298 K, for varying $1\text{Cl}_3:\beta\text{-CD}$ mole ratios, A) 1:4, B) 1:2 and C) 1:0.65. NOE and exchange cross peaks are shown in blue and red respectively. Intensity of the exchange cross peaks decreases with increase in $\beta\text{-CD}$ concentration due to the decrease in population and life time of uncomplexed 1Cl_3 .

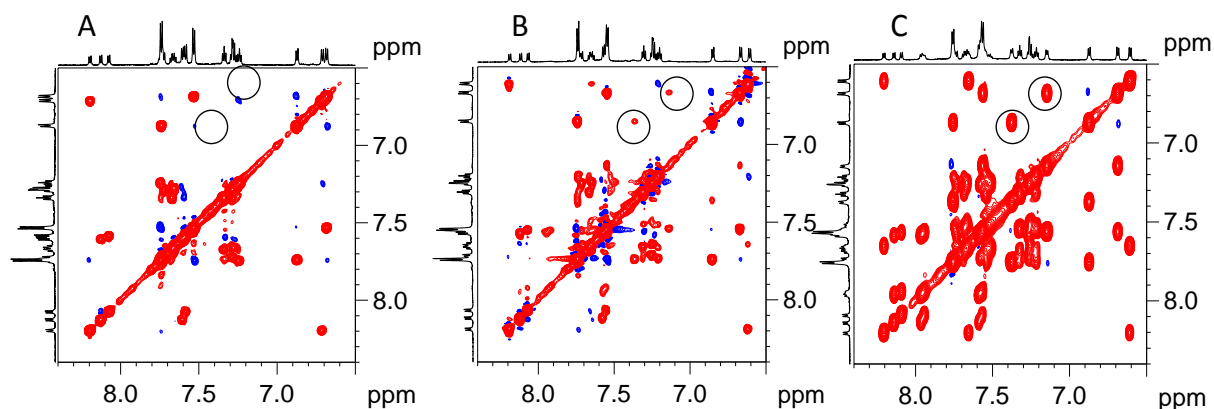


Figure S28. Absorption spectra of 1Cl_3 in solvents of varying polarities.

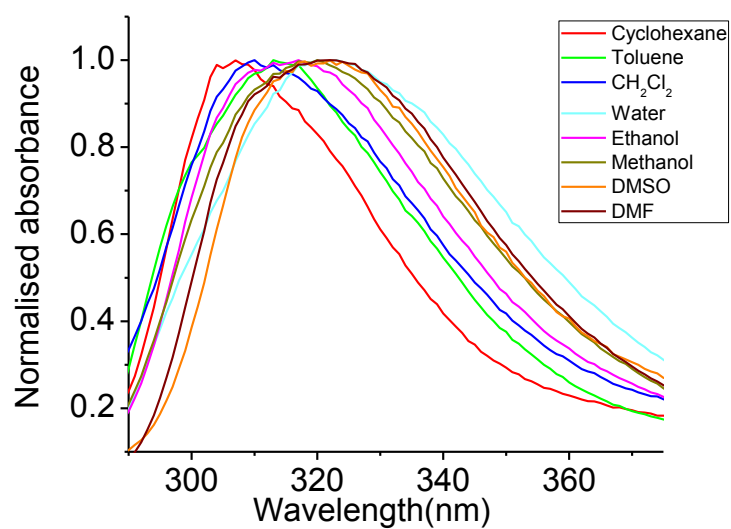


Figure S29. Emission spectra of 1Cl_3 at $\lambda_{\text{ext}}=309$ nm in solvents of varying polarities.

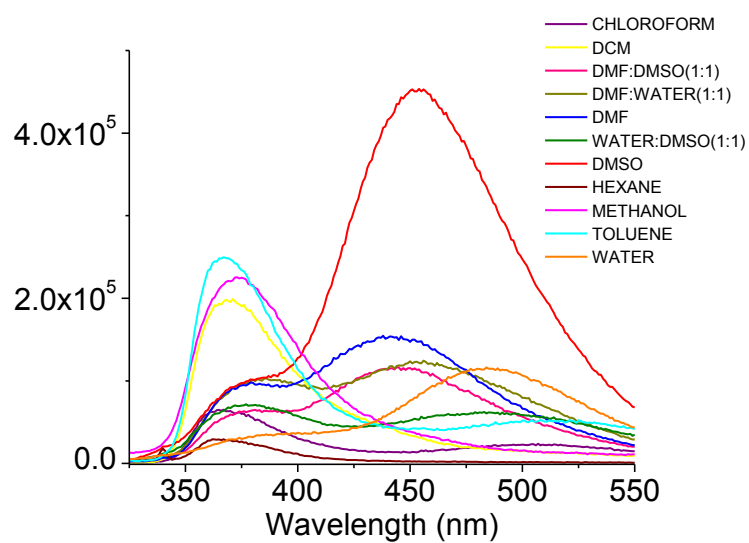


Figure S30. Emission spectra of **1**Cl₃ in aqueous solution with concentration ranging from 1.0×10^{-6} M to 1.0×10^{-4} M

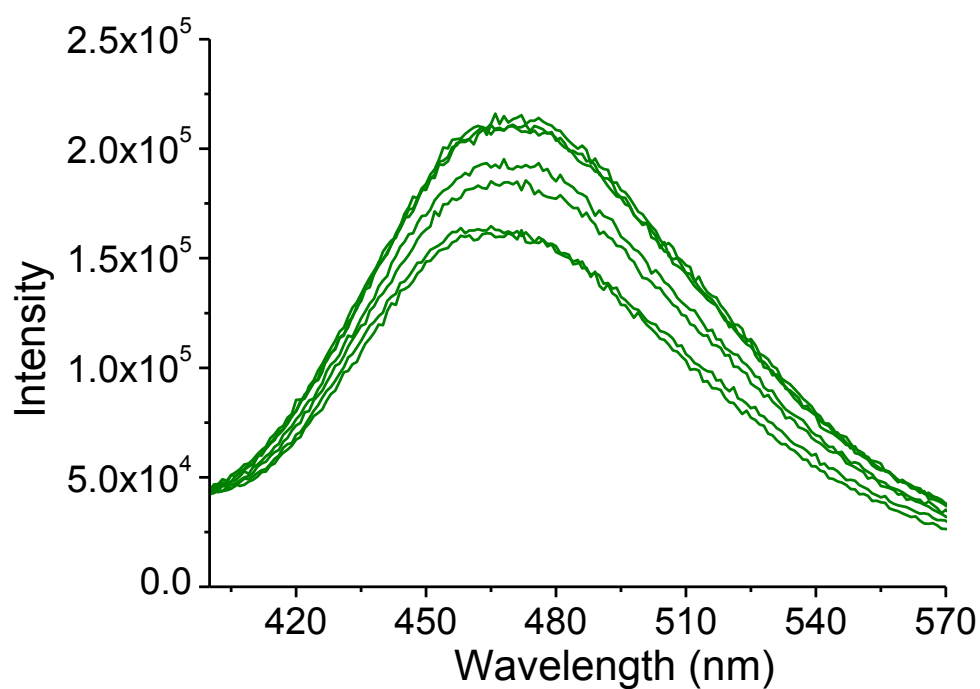


Figure S31. Excitation spectra of **1**Cl₃ in a) hexane and b) water.

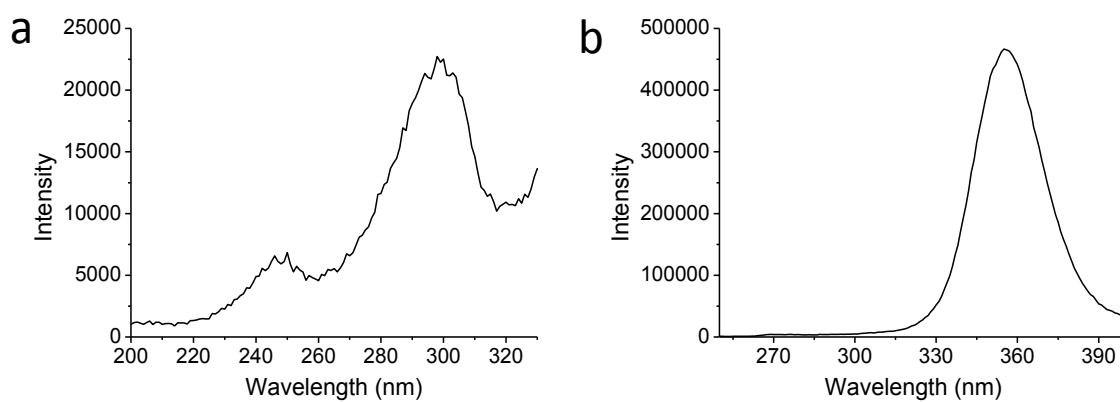


Figure S32. Absorption spectra of 1Cl_3 , $[1\bullet 3\{\text{CB}[7]\}]\text{Cl}_3$ and $[1\bullet\{\beta\text{-CD}\}]\text{Cl}_3$ in aqueous solution at 298K with 1Cl_3 :host mole ratio of 1:3.

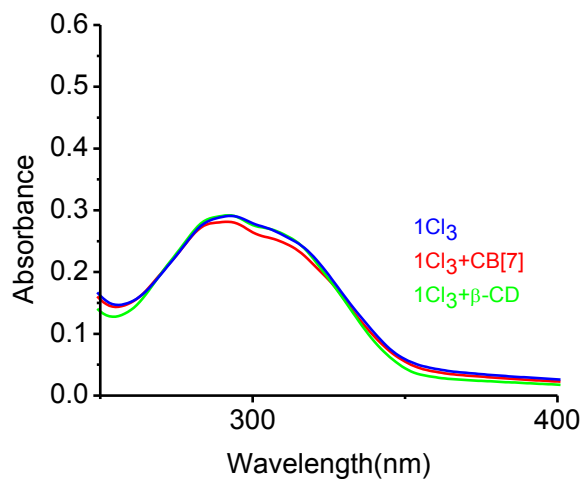
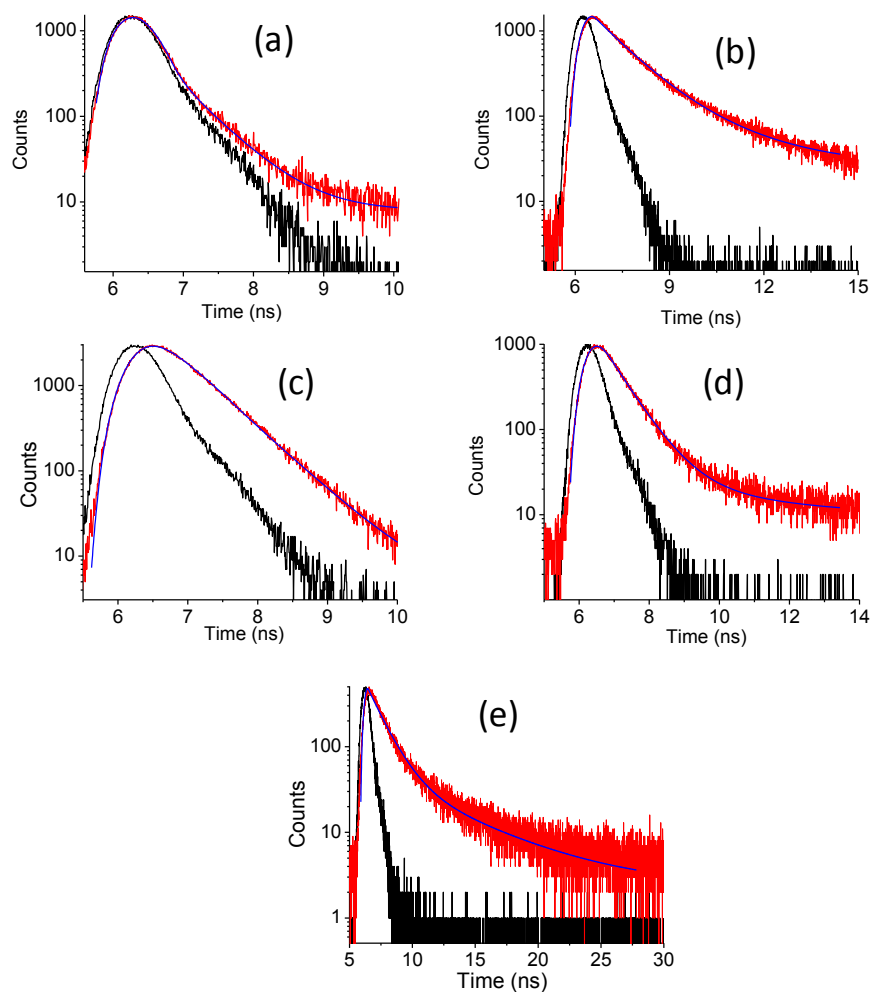


Figure S33. Time dependent fluorescent decay of (a) 1Cl_3 at 388 nm (b) 1Cl_3 at 475 nm (c) $1\text{Cl}_3 + \text{CB}7$ at 388 nm (d) $1\text{Cl}_3 + 3$ equivalents of CB7 at 475 nm (e) $1\text{Cl}_3 + 3$ equivalents of $\beta\text{-CD}$ at 475 nm.



Details Error analyses:

Methodology adopted for evaluating error in preparing solution³ :

Errors to determine the apparent association/dissociation constants K_a/K_d rises due to i) weighing measurements, ii) volume measurement of solvents (to prepare the respective solution, from dilution some error will come) iii) spectrometer based errors (NMR chemical shifts). The error due to weighing the sample arise from instrumental precision. In our lab the instrument error is ± 0.05 mg. So the error to prepare 7.5 mM solution of compound **1Cl₃** was 0.427 % (11.7 mg of **1Cl₃** (the error in weighing was $0.05/11.7 \times 100$) dissolved in 1.8 ml solvent, taken from volumetric pipette). To prepare the corresponding solutions we use 100-1000 μ l pipette (Eppendorf Research micro pipette). For 1000 μ l, the systematic error is ± 6 μ l and random error is ± 2 μ l, for 500 μ l the systematic error is ± 5 μ l and random error is ± 1 μ l. For 400 μ l measurements the the systematic error is ± 5 μ l and random error is ± 1 μ l; while for measuring 100 μ l, the systematic error is ± 3 μ l and random error is ± 0.6 μ l. systematic error is ± 5 μ l and random error is ± 1 μ l; while for measuring 100 μ l, the systematic error is ± 3 μ l and random error is ± 0.6 μ l. To prepare 1.80 ml of 7.50 mM solution we have taken 1000 μ l one time and 400 μ l two times. So the systematic pipette error for measuring 1.00 ml = $[6.00 \times 10^{-6} \text{ L}/(1 \times 10^{-3} \text{ L})] = (0.006)$, i.e. 0.6 %. Systematic error for measuring 0.80 ml = $5.00 \times 10^{-6} \text{ L}/(4.00 \times 10^{-4} \text{ L}) \times 2$, i.e. 2.50 %; The random error for measuring 1.00 ml = $[2.00 \times 10^{-6} \text{ L}/(1 \times 10^{-3} \text{ L})] = (0.002)$, i.e. 0.20 %. and for measuring 0.80 ml = $(1.00 \times 10^{-6} \text{ L}/4.00 \times 10^{-4}) \times 2 \text{ L} = 0.50\%$). Again 0.10 ml of this solution was diluted to 0.50 ml in NMR tube to give the 1.50 mM solution. Therefore, the systematic pipette error for measuring 0.10 ml = $3.00 \times 10^{-6} \text{ L}/1.00 \times 10^{-4} \text{ L}$, i.e. 3.00% and for measuring 0.40 ml is $5.00 \times 10^{-6} \text{ L}/4.00 \times 10^{-4} \text{ L} = 1.25\%$. The random error to measure 0.10 ml = $6.00 \times 10^{-7} \text{ L}/1 \times 10^{-4} \text{ L} = 0.60\%$ and the random error for measuring 0.40 ml = $1.00 \times$

$10^{-6} \text{ L} / 4.00 \times 10^{-4} \text{ L} = 0.25\%$. Thus, the additive systematic error is 7.35 %, while the cumulative random error is 1.55 %.

Methodology adopted to measure spectrometric based errors³:

To calculate the spectrometer-based errors, we prepared 12 independent (1:3) solutions of 1Cl_3 and CB[7] in molar ratio (1:3) in D_2O . Then we investigated the H_i , H_j resonances of 1Cl_3 and H_1 and H_3 resonances of CB[7]. Nearly identical standard deviations were found in each case of the particular taken proton resonance.

SI Table 1. Fraction of complexation (evaluated from NMR integration) for 12 independent solutions having concentration (1:3) molar ratio 1Cl_3 :CB[7] D_2O , 295 K.

Trial	H_i	H_j	H_3	H_1
1	4.657	7.890	5.554	5.809
2	4.655	7.891	5.556	5.807
3	4.654	7.888	5.552	5.805
4	4.658	7.890	5.555	5.804
5	4.659	7.892	5.554	5.806
6	4.658	7.891	5.556	5.808
7	4.656	7.891	5.553	5.809
8	4.659	7.887	5.552	5.806
9	4.656	7.888	5.554	5.807
10	4.660	7.887	5.551	5.808
11	4.655	7.891	5.555	5.809
12	4.656	7.890	5.556	5.807
Average	4.657	7.889	5.554	5.807
Stdv	0.0018	0.0018	0.0017	0.0016

The average percentage standard deviation of 0.2%

As the peak resonances were manually set in this study, so, random error came from the randomly chosen one NMR tube from the twelve solutions and was further examined. Six independent Fourier transformations were taken to calculate the standard deviation. Here also same standard deviations were found in each case of resonance.

SI Table 2. Fraction of complexation for six independent Fourier transformations $\mathbf{1Cl_3:CB[7]}$ (1:3 molar ratio) D_2O at 295 K.

Trial	H_i	H_j	H_3	H_1
1	4.657	7.890	5.554	5.809
2	4.655	7.888	5.552	5.807
3	4.656	7.890	5.553	5.807
4	4.655	7.887	5.554	5.809
5	4.656	7.889	5.552	5.806
6	4.655	7.890	5.552	5.806
Average	4.655	7.889	5.552	5.807
Stdv	0.0008	0.0012	0.0013	0.0014

The average percentage standard deviation of 0.11%

References

- 1) R. R. Ernst, G. Bodenhausen and A. *Principles of NMR in one and two dimensions*. Oxford Univ Press, Oxford, 1987.
- 2) L. Y. Lian, I. L. Barsukov, M. J.; Sutcliffe, K. H. Sze and G. C. K. Roberts. *Methods in Enzymology*, 1994, 239, 857.
- 3) 1. H. W. Gibson, J. W. Jones, L. N. Zakharov, A. L. Rheingold and C. Slebodnick, *Chem. Eur. J.*, 2011, **17**, 3192.